Forward and Inverse Problems: An Exploration of Differential Equations

Matt Charnley

Publication Date

14-12-2023

Forward and Inverse Problems*
An Exploration of Differential Equations

Matt Charnley

April 26, 2013

Abstract

In this paper, both the forward and inverse problems associated with a differential equation are discussed. The theoretical forward problem is developed via solving the Dirichlet problem for the Laplacian in arbitrary domains with smooth boundary, while the inverse problem approach is shown in the example of detecting corroded material on the reverse side of a partially accessible metal plate. Numerical computation of the forward problem with the heat equation was used along with a linearization and regularization method to solve the stated inverse problem, constructing a corrosion profile that approximates the actual corrosion that was used to generate the temperature data. Results will be presented and possibilities for future work will be stated.

*Research started at Rose-Hulman REU 2012, NSF Grant DMS-1003924

Contents

Acknowledgements

Special thanks go out to many people for the development of this work. The work on Inverse Problems was started at the NSF-REU at Rose-Hulman Institute of Technology. Dr. Kurt Bryan (Rose-Hulman), my advisor, and Andrew Rzeznik (Cornell University), my partner for the project, both had a large part in bringing that section of the work together. It would not have happened without their guidance and assistance. Dr. Nancy Stanton (Notre Dame) generated the idea for the forward problem section and provided a great amount of coaching and support in working through the material. She has also been essential in preparing the final version of this paper, and her presence has been invaluable in this effort. Finally, to all of my friends and family who have been with me during this project, thank you for your support over the past year.

1 Introduction and Motivation

Given a generic differential equation with boundary and initial conditions, there are two main ways to set up a problem; either one knows all of the coefficients in the equation and the shape of the boundary, or one knows (part of) the solution to the equation. The first case is the forward problem, which is the problem handled by most differential equations classes. Several different techniques can be used to solve this problem. If the boundary conditions and the geometry of the boundary are simple enough, Fourier series or separation of variables can be used. In other cases, finite element or other numerical methods are necessary to give an approximate solution. In specific cases, like the one discussed in this paper, other analytical methods including Green's functions can be used to give solutions to the forward problem of a differential equation.

The other case, attempting to solve for the boundary of the domain or parameters of a differential equation, is called the inverse problem. In general, an inverse problem occurs when one is trying to deduce the parameters that govern a system from measurements of how that system reacts to certain inputs. For example, if we are given a piece of a graph of a function, and we know the function is a degree 4 polynomial, we can take 5 points off of the graph and back out the coefficients of the polynomial. In this case, we know the form of the solution, *i.e.*

$$f = a_4x^4 + a_3x^3 + a_2x^2 + a_1x + a_0,$$

and based on the value of the function from certain input values, we can deduce the function. This is the process that guides all inverse problems research.

For physical systems, however, the process is much more complicated because as opposed to being governed by a degree 4 polynomial, these systems are governed by differential equations. The inputs to the system are then either initial or boundary conditions, and the data used to recover the system parameters can vary depending on the posed problem. In most cases, for the physical application, one wants to learn about some property of a system that could normally only be accessed by destructive methods, and hopes to use solutions to inverse problems as a way to get this information without destroying the material. For most of the applicable methods used in inverse problems, the differential equations model heat or electricity, neither of which is destructive to a physical object.

In many industrial and engineering applications, it can be useful to know if the reverse side of a partially accessible piece of material has been corroded. This corrosion could damage the efficiency of a system, or make it unsafe to use. Trying to deduce the boundary or internal structure of a region is a common formulation of an inverse problem. Two of the most common differential equations used in physical system analysis via inverse problems are Laplace's equation, $\Delta u = 0$, which governs the flow of electricity in a system, and the heat equation $\frac{\partial u}{\partial t} - \alpha\Delta u = 0$, which governs heat flow. If the reverse side of a piece of material has been damaged, a portion of the material will have different physical properties. This change in properties should alter the overall response of the system to a defined input flux, and the inverse problem tries to construct a relationship between

the temperature or voltage profile of the system and the change in parameters, either where or how it changes.

The field of inverse problems hopes that by taking a mathematical approach to analyzing these situations, it will be possible for a computer to easily reconstruct the structure of the region given a small amount of data. For the particular case considered here, the region is always a rectangular plate of metal, but a portion of the metal is corroded. The data gathered is from the top side of the metal, and the corrosion profile is a function of horizontal position, with support on the bottom side of the plate. With this limited data and a small restriction on what the internal structure of the plate looks like, it is hoped that it will be possible to get an idea of where the plate has been corroded.

What follows is an analysis of both 'problems' that can be associated with a differential equation. The first part, Sections 2 and 3, will discuss the forward problem, and how both a numerical solver and analytic approach can be used to generate solutions. The rest of the paper will show the process of setting up the inverse problem, generating the necessary data, and using it to approximate the corrosion profile of the block of metal. This work was conducted with Andrew Rzeznik (Cornell University) under the direction of Dr. Kurt Bryan at the Rose-Hulman Institute of Technology Summer 2012 REU. Section 4 will discuss the inverse problem of finding the corrosion profile from temperature measurements. Section 5 will cover the process of generating a solution, from the linearization of the problem, use of Green's Identity, and generating a profile with the smallest L^2 norm. Section 6 will discuss different methods used to improve the resulting profiles, and Section 7 will show some of the results. Finally, the paper will close with some conclusions and possibilities for future work in Sections 8 and 9.

1.1 Terms and Definitions

The following terms and symbols will be used frequently through the paper

Ω	The entire region where heat transfer is taking place.
Ω_1	The section of Ω where the material has not been corroded.
Ω_2	The section of Ω where the material has been corroded.
u_0	The temperature profile in the uncorroded plate Ω made of material (1), using the same input flux used to compute u_1, u_2.
u_1	The temperature profile in Ω_1, function of (x, y, t).
u_2	The temperature profile in Ω_2, function of (x, y, t).
$C(x)$	The corrosion profile; The function of the curve that separates Ω_1 from Ω_2.
α	Thermal Diffusivity, a material property. Determines how fast heat can diffuse through the medium.
α_i	Thermal Diffusivity for material i, which is present in region Ω_i.
k	Thermal Conductivity, a material property. Determines how well heat can be conducted in from the environment.
k_i	Thermal Conductivity for material i, which is present in region Ω_i.

2 Forward Problem

In order to directly contrast with the inverse problem that will be discussed in Section 4, assume that we have a finite rectangle Ω of length L and height 1, as shown in Figure 2.1. The rectangle Ω is set in the Cartesian plane $\mathbb{R}^2$ so that $x = 0$ marks the left side of the rectangle, $x = L$ is at the right edge, $y = 0$ denotes the bottom of the sample and $y = 1$ indicates the top.

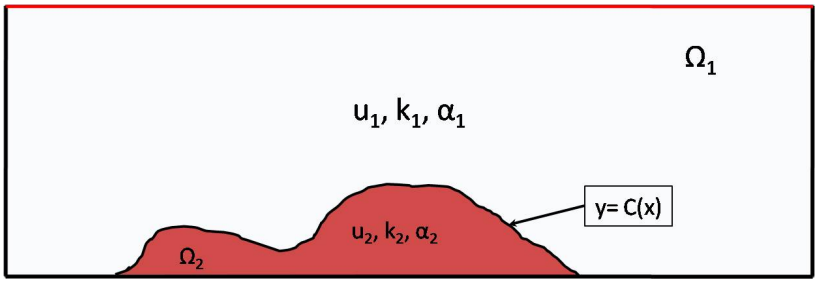

Figure 2.1: General Setup for the Problem

The forward problem is what is usually solved in differential equations classes: given the boundary and initial conditions on the problem, solve for the temperature profile. For this specific problem, we know there are two regions, separated by the curve $C(x)$, and each region has different thermal properties, such as thermal conductivity and thermal diffusivity. We will also assume that all external boundaries are insulated except for the one at $y = 1$, where some input flux $g(x)$ is applied. We also know that the temperature and heat flux must be continuous over any interface, including the curve $C(x)$. All of these conditions can be formally stated as follows.

We assume that u_1 satisfies

$$\begin{aligned} \frac{\partial u_1}{\partial t} - \alpha_1 \Delta u_1 &= 0 \text{ on } \Omega_1, \\ \frac{\partial u_1}{\partial x} &= 0 \text{ on } x = 0,\ x = L, \\ \frac{\partial u_1}{\partial y} &= g(x) \text{ on } y = 1, \\ u_1(x, y, 0) &= 0 \text{ on } \Omega_1, \end{aligned}$$

while it is assumed that u_2 satisfies

$$\begin{aligned} \frac{\partial u_2}{\partial t} - \alpha_2 \Delta u_2 &= 0 \text{ on } \Omega_2, \\ \frac{\partial u_2}{\partial x} &= 0 \text{ on } x = 0,\ x = L, \\ \frac{\partial u_2}{\partial y} &= 0 \text{ on } y = 0, \\ u_2(x, y, 0) &= 0 \text{ on } \Omega_2, \end{aligned}$$

and the continuity conditions on $C(x)$ give us

$$\begin{aligned} u_1 &= u_2 \text{ on } C(x), \\ k_1 \frac{\partial u_1}{\partial \vec{n}} &= k_2 \frac{\partial u_2}{\partial \vec{n}} \text{ on } C(x). \end{aligned}$$

The forward problem would be stated: Given the input flux $g(x)$, the thermal properties of both materials, and the curve $C(x)$ dividing Ω_1 and Ω_2, find the temperature profiles u_1 and u_2 satisfying these equations.

If the domain is simple, *e.g.* a rectangle, Fourier series and separation of variables can be used to solve this problem. As discussed in section 3, multiple analytical methods exist for solving the Dirichlet problem for the Laplacian, and in a similar way, the heat equation, in an arbitrary region with given boundary conditions. However, for more complicated boundaries, particularly in the case of corrosion, it becomes easier and faster to carry out the computations numerically. COMSOL Multiphysics was our program of choice for solving the forward heat equation problem numerically. It uses a finite element method to generate the solution to the heat equation given a geometry and any specified combination of heat fluxes, insulations and material properties. From this data, it will generate the temperature values for a mesh of points (x, y) in the plate at a set of specified timesteps. The program also contains a functionality to export different sections of the data to text files, which can be used in MATLAB or other numerical software.

3 The Laplacian: Solutions to the Dirichlet Problem

Assume we have a bounded region $\Omega \subset \mathbb{R}^n$ with smooth boundary $\partial\Omega$. In most of the methods that follow, the assumptions of a smooth boundary can be relaxed with additional analysis. For example, solving the Dirichlet problem for the Laplacian in bounded domains using Brownian Motion allows this constraint to be relaxed to a *regular* boundary, which is closer to a continuous boundary. See section 2.3 of [4] for more information on this approach.

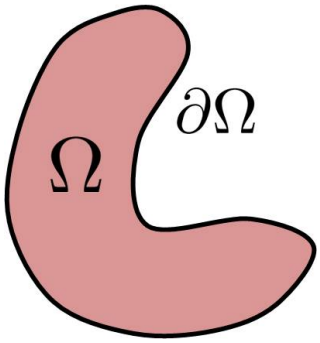

Figure 3.1: Schematic of a Sample Region Ω in $\mathbb{R}^2$.

We would like to solve the Dirichlet problem for the Laplacian on the domain Ω, *i.e.*, given functions f on Ω and g on $\partial\Omega$, we want to find a function u on Ω such that

$$\Delta u = f \ \text{ on } \Omega \qquad u = g \ \text{ on } \partial\Omega. \tag{3.1}$$

We can also split this problem into two disjoint problems, which we will construct solutions for separately. We will find u_1 and u_2 on Ω satisfying

$$\Delta u_1 = f \ \text{ on } \Omega \qquad u_1 = 0 \ \text{ on } \partial\Omega.$$

$$\Delta u_2 = 0 \ \text{ on } \Omega \qquad u_2 = g \ \text{ on } \partial\Omega.$$

so that $u = u_1 + u_2$ solves the original Dirichlet Problem (3.1). The construction of the solution will follow Chapter 2 of Folland [3].

3.1 Definitions

This first section covers a few definitions that will be used frequently in the proofs that follow. The following table lists the notation for the different spaces that will be used.

Notation	Definition
$C(\Omega)$	Continuous Functions on Ω
$C^k(\Omega)$	k-times continuously differentiable functions on Ω.
$C^\infty(\Omega)$	Smooth functions on Ω
$C_c^\infty(\Omega)$	Smooth functions on Ω with compact support
$L^p(\Omega)$	Space of functions satisfying $\|\|f\|\|_p = (\int_\Omega \|f\|^p)^{1/p} < \infty$
$B_r(x)$	The ball of radius r centered at x, $\{y \in \mathbb{R}^n : \|\|y - x\|\| < r\}$
$S_r(x)$	The sphere of radius r centered at x, $\{y \in \mathbb{R}^n : \|\|y - x\|\| = r\}$
ω_n	The volume of the unit sphere in $\mathbb{R}^n$

Definition 3.1 (Multi-index)**.** A **multi-index** α is a set $\alpha = (\alpha_1, ..., \alpha_n)$ with $\alpha_i \in \mathbb{N}$ that can act on elements and functions on $\mathbb{R}^n$

- $|\alpha| = \alpha_1 + \alpha_2 + \cdots + \alpha_n$
- $x^\alpha = x_1^{\alpha_1} x_2^{\alpha_2} \cdots x_n^{\alpha_n}$
- $\partial^\alpha = \frac{\partial^{\alpha_1}}{\partial x_1^{\alpha_1}} \frac{\partial^{\alpha_2}}{\partial x_1^{\alpha_2}} \cdots \frac{\partial^{\alpha_n}}{\partial x_1^{\alpha_n}}$

Definition 3.2 (Convergence in $C_c^\infty(\Omega)$)**.** A sequence ϕ_j **converges to** ϕ **in** $C_c^\infty(\Omega)$ if all of the ϕ_j are supported in a common compact subset of Ω and $\partial^\alpha \phi_j \to \partial^\alpha \phi$ uniformly for every multi-index α.

Definition 3.3. If u is a linear functional on $C_c^\infty(\Omega)$, then we denote the image of applying u to $\phi \in C_c^\infty(\Omega)$ by $\langle u, \phi \rangle$.

Definition 3.4 (Distribution)**.** A **distribution** on Ω is a linear functional u on $C_c^\infty(\Omega)$ that is continuous in the sense that if $\phi_j \to \phi$ in $C_c^\infty(\Omega)$, then $\langle u, \phi_j \rangle \to \langle u, \phi \rangle$.

Example 1. Distributions are generalized functions.

- Any locally integrable function f can be considered a distribution using the inner product operation, which is well-defined because ϕ has compact support:

$$\langle f, \phi \rangle = \int f \overline{\phi}.$$

- Any locally finite measure, μ, is also a distribution by the formula

$$\langle \mu, \phi \rangle = \int \phi \, d\mu.$$

We would like to be able to apply linear operators, specifically linear differential operators, to distributions so we can use them to help solve differential equations. Let T be a linear operator on $C_c^\infty(\Omega)$ that is continuous in the sense that if $\phi_j \to \phi$, then $T\phi_j \to T\phi$.

If there is another operator T^* such that

$$\int (T\phi)\psi = \int \phi(T^*\psi) \qquad \forall\, \phi, \psi \in C_c^\infty(\Omega),$$

then we can have T act on distributions by the formula

$$\langle Tu, \phi \rangle = \langle u, T^*\phi \rangle.$$

T^* is the **dual**, or **transpose**, of T. It can be shown, via integration by parts, that if $T = \partial^\alpha$, then $T^* = (-1)^{|\alpha|}\partial^\alpha$. Therefore, if we are looking at the Laplacian operator,

$$(\Delta)^* = \sum_{j=1}^{n} \left(\frac{\partial^2}{\partial x_j^2} \right)^* = \sum_{j=1}^{n} (-1)^2 \frac{\partial^2}{\partial x_j^2} = \Delta,$$

and we get the following definition for finding distributional solutions to Poisson's equation.

Definition 3.5. If u is a distribution on $C_c^\infty(\Omega)$, then $\Delta u = f$ in the sense of distributions if $\forall\, \phi \in C_c^\infty(\Omega)$

$$\langle f, \phi \rangle = \langle u, \Delta\phi \rangle.$$

This is the main definition that will be used in the development of solutions of boundary value problems for the Laplacian.

We also state a few theorems that will be used to prove some of the points within this paper.

Theorem 3.1 ([3] 0.10, Generalized Young's Inequality)**.** *Let $(X,\ \mu)$ be a σ-finite measure space, and let $1 \le p \le \infty$ and $C > 0$. suppose K is a measurable function on $X \times X$ such that*

$$\sup_{x \in X} \int_X |K(x,y)|\ d\mu(y) \le C \qquad \sup_{y \in X} \int_X |K(x,y)|\ d\mu(x) \le C.$$

If $f \in L^p(X)$, the function Tf defined by

$$Tf(x) = \int_X K(x,y) f(y)\ d\mu(y)$$

is well-defined almost everywhere and is in $L^p(X)$, and $||Tf||_p \le C||f||_p$.

Theorem 3.2 ([3] 0.13, Approximation to the Identity)**.** *Suppose $\phi \in L^1$ and $\int \phi(x)\ dx = a$. For each $\epsilon > 0$, define the function ϕ_ϵ by $\phi_\epsilon(x) = \epsilon^{-n}\phi(\epsilon^{-1}x)$. If $f \in L^p$, $1 \le p < \infty$, then $f * \phi_\epsilon \to af$ in the L^p norm as $\epsilon \to 0$. If $f \in L^\infty$ and f is uniformly continuous on a set V then $f * \phi_\epsilon \to af$ uniformly on V as $\epsilon \to 0$.*

Definition 3.6 (Hypoelliptic)**.** A differential operator L with C^∞ coefficients is called **hypoelliptic** if any distribution u on an open set Ω such that Lu is C^∞ on Ω, must itself be C^∞ on Ω.

Theorem 3.3 ([3] 1.58)**.** *If L is a differential operator with constant coefficients, the following are equivalent:*

1. *Some fundamental solution for L is C^∞ on $\mathbb{R}^n \setminus \{0\}$.*
2. *Every fundamental solution for L is C^∞ on $\mathbb{R}^n \setminus \{0\}$.*
3. *L is hypoelliptic.*

Corollary 1 ([3] 2.20)**.** *Δ is hypoelliptic,* i.e. *every distribution solution of $\Delta u = 0$ is a harmonic function.*

Remark. This corollary follows from derivation of the fundamental solution in section 3.3 and applying Theorem 3.3.

3.2 Dirichlet's Principle

For Ω a bounded domain with smooth boundary, define the Hermitian Form $D : C^1(\Omega) \times C^1(\Omega) \to \mathbb{R}$ by

$$D(u, v) = \int_\Omega \nabla u \cdot \overline{\nabla v}.$$

$D(u, u) = \int_\Omega |\nabla u|^2$ is the Dirichlet Integral of u.

The functional $||u|| = D(u, u)^{1/2}$ is a seminorm on $C^1(\Omega)$, since it satisfies the triangle inequality, but all functions that are constant on each connected component of Ω will map to 0.

Define the function space $H_1(\Omega)$ as the completion of $C^1(\overline{\Omega})$ with respect to the norm

$$||u||_{(1)} = \left[D(u, u) + \int_\Omega |u|^2 \right]^{1/2}.$$

This space can be regarded as a subspace of L^2 of functions, all of whose derivatives are still in L^2. It is a Hilbert Space with inner product

$$\langle u, v \rangle = D(u, v) + \int_\Omega u\overline{v}.$$

Theorem 3.4 ([3] 2.39)**.** *If $u \in C^1(\overline{\Omega})$, then the restriction of u to $S = \partial\Omega$ is in $L^2(S)$, and $\exists\, C > 0$ such that*

$$\int_S |u|^2 \leq C||u||^2_{(1)} \quad \forall\, u \in C^1(\overline{\Omega}).$$

Proof. Let ν be the normal vector on S. Extend ν to be a vector field on $\overline{\Omega}$ by making it constant in a small neighborhood of S, and multiplying it by a smooth cutoff function. Then

$$\int_S |u|^2 = \int_S (|u|^2 \nu) \cdot \nu = \sum_{j=1}^n \int_\Omega \partial_j (|u|^2 \nu_j),$$

where the last step is by the Divergence Theorem.

Using the fact that $|u|^2 = u\overline{u}$ and applying the product rule gives

$$\begin{aligned}\int_S |u|^2 &\leq \sum_{j=1}^{n} \int_\Omega |(\partial_j u)\overline{u}\nu_j| + |u(\partial_j \overline{u})\nu_j| + |u\overline{u}\partial_j \nu_j| \\ &\leq \sum_{j=1}^{n} \int_\Omega |(\partial_j u)\overline{u}|\,|\nu_j| + |u(\partial_j \overline{u})|\,|\nu_j| + |u\overline{u}|\,|\partial_j \nu_j|.\end{aligned}$$

Defining $C' = \sup_\Omega \sum_{j=1}^{n} (|\nu_j| + |\partial_j \nu_j|)$ we can bound all of the terms containing ν to get

$$\int_S |u|^2 \leq C' \sum_{j=1}^{n} \int_\Omega |(\partial_j u)\overline{u}| + |u(\partial_j \overline{u})| + |u|^2.$$

Applying the Cauchy-Schwarz inequality and using that $2ab \leq a^2 + b^2 \;\forall\, a, b \in \mathbb{R}$ gives

$$\begin{aligned}\int_S |u|^2 &\leq C' \left(2 \sum_{j=1}^{n} \left[\int_\Omega |u|^2 \right]^{1/2} \left[\int_\Omega |\partial_j u|^2 \right]^{1/2} + n \int_\Omega |u|^2 \right) \\ &\leq C' \left(n \int_\Omega |u|^2 + \sum_{j=1}^{n} \int_\Omega |\partial_j u|^2 + n \int_\Omega |u|^2 \right).\end{aligned}$$

Finally, since $|\partial_j u|^2 \leq \sum_{i=1}^{n} |\partial_i u|^2 = |\nabla u|^2$ for each j, this reduces to

$$\int_S |u|^2 \leq C' \left(2n \int_\Omega |u|^2 + n \int_\Omega |\nabla u|^2 \right) \leq 2nC' ||u||^2_{(1)}.$$

So, taking $C = 2nC'$ gives the desired conclusion. ■

From this result, we get:

Corollary 2 ([3] 2.40)**.** *The restriction map $u \mapsto u|_S$ from $C^1(\overline{\Omega})$ to $C^1(S)$ extends continuously to a map from $H_1(\Omega)$ to $L^2(S)$.*

This corollary holds because $C^1(\overline{\Omega})$ is dense in $H_1(\Omega)$ and $C^1(S)$ is dense in $L^2(S)$.

This tells us that elements of $H_1(\Omega)$ have boundary elements that are well-defined as elements of $L^2(S)$.

Define the space $H_1^0(\Omega)$ as the closure of $C_c^\infty(\Omega)$ in $H_1(\Omega)$. If $f \in H_1^0(\Omega)$, then $f|_S = 0$, since the function f is the limit of functions that are compactly supported within Ω. Since each of these functions must vanish on the boundary of Ω, so must f.

Assume that we want to solve the Dirichlet problem

$$\Delta w = 0 \text{ on } \Omega \qquad w = g \text{ on } S, \tag{3.2}$$

and assume that $g = f|_S$ where $f \in H_1(\Omega)$. If $w - f \in H_1^0(\Omega)$, then $w - f$ vanishes on the boundary of Ω, so w approaches f on S. Since $g = f|_S$, we will take this to mean that $w = g$ on S. Thus, we can solve this form of the Dirichlet Problem by finding a harmonic function w such that $w - f \in H_1^0(\Omega)$.

Theorem 3.5 ([3] 2.41)**.** *If $w \in H_1(\Omega)$, then w is harmonic in Ω if and only if w is orthogonal to $H_1^0(\Omega)$ with respect to D.*

Proof. Take any $w \in C^1(\overline{\Omega})$ and $v \in C_c^\infty(\Omega)$. By Green's Identity, we know that

$$\int_S w \partial_\nu \overline{v} = \int_\Omega w\overline{\Delta v} + \nabla w \cdot \overline{\nabla v}.$$

However, v vanishes at the boundary, so

$$\int_\Omega w\overline{\Delta v} = -\int_\Omega \nabla w \cdot \overline{\nabla v} = -D(w, v).$$

By taking limits, this relation also holds for $w \in H_1(\Omega)$. Then, using Definition 3.5, along with Theorem 3.3 and Corollary 1, we have

$$\begin{aligned} w \text{ harmonic in } \Omega &\Leftrightarrow \Delta w = 0 \text{ in the sense of distributions} \\ &\Leftrightarrow 0 = \langle w, \Delta v \rangle = \int_\Omega w\overline{\Delta v} \ \ \forall\, v \in C_c^\infty(\Omega) \\ &\Leftrightarrow D(w, v) = 0 \ \forall\, v \in C_c^\infty(\Omega) \\ &\Leftrightarrow D(w, v) = 0 \ \forall\, v \in H_1^0(\Omega) \end{aligned}$$

which is the definition of being orthogonal to $H_1^0(\Omega)$. ∎

If we take the space $H_1(\Omega)$ and mod out by the kernel of the Hermitian form D, we get a Hilbert Space on which D is a norm. Within this space, we also have $H_1^0(\Omega)$ as a closed subspace, and $H_1^0(\Omega)^\perp$ is the set of harmonic functions on Ω.

So, based on the properties of Hilbert Spaces, for each $f \in H_1(\Omega)$, there is a unique decomposition $f = w + v$, where w is harmonic in Ω, and $v \in H_1^0(\Omega)$. Therefore, given f with $f|_S = g$, the orthogonal projection w of f onto the harmonic functions is the solution of the given Dirichlet problem.

However, in this space of functions, we know D is a norm, and, in a Hilbert Space, if $f = w + v$ and w and v belong to orthogonal sets, the orthogonal projections of f onto each set minimize the norm of both w and v. From this, we get Dirichlet's Principle.

Theorem 3.6 (Dirichlet's Principle)**.** *If f, $w \in H_1(\Omega)$, the following are equivalent.*

1. *w is harmonic and $w - f \in H_1^0(\Omega)$.*
2. *$D(w,w) \leq D(u,u)\ \forall\, u \in H_1(\Omega)$ with $u - f \in H_1^0(\Omega)$.*
3. *$D(w-f, w-f) \leq D(u,u)\ \forall\, u \in H_1(\Omega)$ with $u - f$ harmonic in Ω.*

So, by minimizing these norms, we are able to solve the Dirichlet problem (3.2), where boundary values are taken in the sense of Corollary 2.

3.3 Fundamental Solution

In order to attack this problem from a different angle, we seek to find a fundamental solution for the Laplacian. This will give us a way to compute some solutions of Laplace's and Poisson's equation, and will go into the development of the Green's functions in Section 3.4.

Definition 3.7 (Fundamental Solution)**.** A **Fundamental Solution** to a differential operator L is a distribution K such that $LK = \delta$, which is the point mass at the origin, *i.e.*, $\forall\, \phi \in C^\infty$

$$\langle LK, \phi \rangle = \langle \delta, \phi \rangle = \phi(0).$$

Remark. If $f \in C_c^\infty$, then $u = K * f$ solves

$$Lu = L(K * f) = (LK) * f = \delta * f = f.$$

To begin, we cite the Malgrange-Ehrenpreis Theorem, which tells us that Δ will have a fundamental solution.

Theorem 3.7 ([3] 1.56, Malgrange-Ehrenpreis)**.** *Every differential operator L with constant coefficients has a fundamental solution.*

We now look to find this fundamental solution for Δ. Since Δ commutes with rotations, this fundamental solution should be radial and harmonic on $\mathbb{R}_n \setminus \{0\}$.

Proposition 1 ([3] 2.2)**.** *If f is radial,* i.e. *$f(x) = \phi(r) = \phi(|x|)$, then*

$$\Delta f(x) = \phi''(r) + \frac{n-1}{r}\phi'(r).$$

Corollary 3 ([3] 2.3)**.** *If f is radial, then $\Delta f = 0$ on $\mathbb{R}^n \setminus \{0\}$ if and only if $\phi(r) = a + br^{2-n}$ $(n \neq 2)$ or $\phi(r) = a + b\log r$ $(n = 2)$, where a and b are constants.*

Consider the case $n \neq 2$. Since Δ applied to any constant is zero, we can ignore the constant term in the expression. So we are looking for a function of the form $N(x) = b|x|^{2-n}$ that satisfies $\Delta N = \delta$. In the sense of distributions, we want to show that

$$\phi(0) = \langle \Delta N, \phi \rangle = \langle N, \Delta\phi \rangle \qquad \forall\, \phi \in C_c^\infty$$

Theorem 3.8 ([3] 2.17, Fundamental Solution of the Laplacian)**.** *Set*

$$N(x) = \frac{|x|^{2-n}}{(2-n)\omega_n} \ (n \neq 2) \quad or \quad N(x) = \frac{1}{2\pi} \log |x| \ (n = 2)$$

Then N is a fundamental solution for Δ

Proof 1. Using Green's Identities. Consider the case $n \neq 2$.

Take any $\phi \in C_c^\infty$. Define $\Omega = B_r(0) \setminus B_\epsilon(0)$, removing a small ball around the origin, where r has been chosen such that the support of ϕ is contained in $B_r(0)$.

Then

$$\begin{aligned}
\int_\Omega N\Delta\phi \ dx &= \int_\Omega N\Delta\phi - \phi\Delta N \ dx \\
&= \int_{\partial\Omega} N\partial_\nu\phi - \phi\partial_\nu N \ d\sigma \\
&= \int_{S_r(0)} N\partial_\nu\phi - \phi\partial_\nu N \ d\sigma + \int_{S_\epsilon(0)} N\partial_\nu\phi - \phi\partial_\nu N \ d\sigma
\end{aligned}$$

where the first line uses the fact that N is harmonic in Ω, and Green's Identity is applied to get to the second line.

Since N is of the form $b|x|^{2-n}$, taking the outward normal of the sphere gives that on $S_\rho(0)$.

$$\begin{aligned}
N &= b\rho^{2-n} \\
\partial_\nu N &= b(2-n)\rho^{1-n} \\
\partial_\nu\phi &= \nu \cdot \nabla\phi = \frac{1}{\rho}\sum x_j\partial_j\phi
\end{aligned}$$

Plugging this in with $\rho = r$ and $\rho = \epsilon$, gives

$$\int_\Omega N\Delta\phi \ dx = \int_{S_r(0)} br^{2-n}\partial_\nu\phi - \phi \cdot b(2-n)r^{1-n} \ d\sigma + \int_{S_\epsilon(0)} b\epsilon^{2-n}\partial_\nu\phi + \phi \cdot b(2-n)\epsilon^{1-n} \ d\sigma$$

However, since the support of ϕ is contained in $B_r(0)$, both ϕ and $\partial_\nu\phi$ are identically zero on $S_r(0)$. So the first integral vanishes and we are left with

$$\begin{aligned}
\int_\Omega N\Delta\phi \ dx &= \int_{S_\epsilon(0)} b\epsilon^{2-n}\frac{1}{\epsilon}\sum_{j=1}^n x_j\partial_j\phi + \phi \cdot b(2-n)\epsilon^{1-n} \ d\sigma \\
&= \frac{b}{\epsilon^{n-1}}\int_{S_\epsilon(0)} \sum_{j=1}^n x_j\partial_j\phi + \phi(2-n) \ d\sigma \\
&= b\omega_n\left[\frac{1}{\epsilon^{n-1}\omega_n}\int_{S_\epsilon(0)}\sum_{j=1}^n x_j\partial_j\phi \ d\sigma + \frac{2-n}{\epsilon^{n-1}\omega_n}\int_{S_\epsilon(0)} \phi \ d\sigma\right]
\end{aligned}$$

Then, sending ϵ to zero gives that

$$\begin{aligned}
\langle N, \Delta\phi\rangle &= \int_{\mathbb{R}^n} N\Delta\phi = \lim_{\epsilon\to 0}\int_\Omega N\Delta\phi \\
&= \lim_{\epsilon\to 0} b\omega_n\left[\frac{1}{\epsilon^{n-1}\omega_n}\int_{S_\epsilon(0)}\sum_{j=1}^n x_j\partial_j\phi\ d\sigma + \frac{2-n}{\epsilon^{n-1}\omega_n}\int_{S_\epsilon(0)}\phi\ d\sigma\right] \\
&= b\omega_n\left[\lim_{\epsilon\to 0}\frac{1}{\epsilon^{n-1}\omega_n}\int_{S_\epsilon(0)}\sum_{j=1}^n x_j\partial_j\phi\ d\sigma + \lim_{\epsilon\to 0}\frac{2-n}{\epsilon^{n-1}\omega_n}\int_{S_\epsilon(0)}\phi\ d\sigma\right] \\
&= b\omega_n[0 + (2-n)\phi(0)] = b(2-n)\omega_n\phi(0)
\end{aligned}$$

where the expression is simplified in the last line because the average value of ϕ on $S_\epsilon(0)$,

$$\frac{1}{\epsilon^{n-1}\omega_n}\int_{S_\epsilon(0)}\phi\ d\sigma \to \phi(0)$$

as $\epsilon \to 0$. Also, since ϕ and $\partial\phi$ are continuous, they are bounded as $\epsilon \to 0$, and $\sum x_j\partial_j\phi$ is of order ϵ as ϵ goes to zero, so that integral vanishes.

Since we want $\langle N, \Delta\phi\rangle = \phi(0)$, we set $b = \frac{1}{(2-n)\omega_n}$, giving

$$N(x) = \frac{|x|^{2-n}}{(2-n)\omega_n}$$

as the fundamental solution. ■

Another proof of the fundamental solution for Δ uses some notation that will be employed later, so it will be shown here.

Proof 2. Smoothed Functions. Consider the case $n \neq 2$.

Define

$$N^\epsilon(x) = \frac{(|x|^2+\epsilon^2)^{(2-n)/2}}{(2-n)\omega_n}.$$

$N^\epsilon \to N$ pointwise as $\epsilon \to 0$, and N^ϵ are all dominated by a locally integrable function ($|N|$) as $\epsilon \to 0$, so by the dominated convergence theorem $N^\epsilon \to N$ in the topology of distributions. Therefore, we need to show that

$$\Delta N^\epsilon \to \delta \quad \text{or} \quad \langle \Delta N^\epsilon, \phi\rangle \to \phi(0)\ \ \forall\, \phi \in C_c^\infty \quad \text{as } \epsilon \to 0$$

Calculation shows that

$$\Delta N^\epsilon(x) = \frac{n}{\omega_n}\epsilon^2(|x|^2+\epsilon^2)^{-(n+2)/2} = \epsilon^{-n}\psi(\epsilon^{-1}x)$$

where

$$\psi(x) = \Delta N^1(x) = \frac{n}{\omega_n}(|x|^2+1)^{-(n+2)/2}.$$

Since the function is radial $\Delta N^\epsilon(-x) = \Delta N^\epsilon(x)$ and

$$\langle \Delta N^\epsilon, \phi\rangle = \int \Delta N^\epsilon(x)\phi(x)\ dx = \int \Delta N^\epsilon(-x)\phi(x)\ dx = \phi * \Delta N^\epsilon(0) \to a\phi(0)$$

where $a = \int \psi(x)\ dx$ by approximations to the identity (Theorem 3.2). However, integration in polar coordinates gives

$$\int \psi(x)\ dx = n\int_0^\infty (r^2+1)^{-(n+2)/2} r^{n-1}\ dr = \frac{n}{2}\int_0^1 s^{(n-2)/2}\ ds = 1$$

by the substitution $s = \frac{r^2}{r^2+1}$.

Therefore $\langle \Delta N^\epsilon, \phi\rangle \to \phi(0)$, and N is a fundamental solution of Δ. ■

3.4 Green's Function

Assume that we have a bounded domain Ω, with smooth boundary S.

In order to define the Green's Function, the following notation will be used for the fundamental solution N developed in the previous section.

$$\begin{aligned} N(x,y) &:= N(x-y) \\ N^\epsilon(x,y) &:= N^\epsilon(x-y) \end{aligned}$$

Definition 3.8 (Green's Function)**.** The **Green's Function** for the Laplacian is a function $G(x,y)$ on $\Omega \times \overline{\Omega}$ satisfying

- $G(x,\cdot) - N(x,\cdot)$ is harmonic on Ω and continuous on $\overline{\Omega}$, where N is the fundamental solution of the Laplacian.
- $G(x,y) = 0\ \forall\, x \in \Omega,\ y \in S$.

G is unique, because, $\forall\, x \in \Omega$, it is the solution to the Dirichlet problem in Ω with $G(y) = -N(x,y)$, and by ([3] 2.15), this solution is unique. So, if we can solve the Dirichlet problem and get continuous solution data, we can find the Green's function. Conversely, if we have the Green's function, we have simple solutions to the Dirichlet problem, as will be shown below. The first theorem below, which we will not give a proof of, states that the Green's function does exist for any bounded domain with smooth boundary. Given this information, we will then prove that the Green's function is symmetric.

Theorem 3.9 ([3] 2.35)**.** *Ω is a bounded domain and $S = \partial\Omega$ is C^∞. Then G exists and $\forall\, x \in \Omega$, $G(x,\cdot)$ is C^∞ on $\overline{\Omega} \setminus \{x\}$*

Theorem 3.10 ([3] 2.36)**.** $G(x,y) = G(y,x)\ \forall\, x, y \in \Omega$

Proof. Define two functions

$$u(z) = G(x,z) - N(x,z) + N^\epsilon(x,z) \qquad v(z) = G(y,z) - N(y,z) + N^\epsilon(y,z)$$

Since $G - N$ is harmonic in the second coordinate by the definition of the Green's Function,

$$\Delta u(z) = \Delta N^\epsilon(x,z) \qquad \Delta v(z) = \Delta N^\epsilon(y,z)$$

Green's Second Identity tells us that

$$\int_\Omega u\Delta v - v\Delta u = \int_S u\partial_{\nu_z} v - v\partial_{\nu_z} u$$

The left hand side of this expression simplifies to

$$\begin{aligned}\int_\Omega u\Delta v - v\Delta u &= \int_\Omega u(z)\Delta N^\epsilon(y,z) - v(z)\Delta N^\epsilon(x,z) \\ &= \int_\Omega u(z)\Delta N^\epsilon(y-z)\ dz - \int_\Omega v(z)\Delta N^\epsilon(x-z)\ dz \\ &= u * \Delta N^\epsilon(y) - v * \Delta N^\epsilon(x)\end{aligned}$$

And the right hand side, since G is zero on the boundary,

$$\begin{aligned}\int_S u\partial_{\nu_z} v - v\partial_{\nu_z} u &= \int_S \left[G(x,z) - N(x,z) + N^\epsilon(x,z)\right]\partial_{\nu_z} v - \left[G(y,z) - N(y,z) + N^\epsilon(y,z)\right]\partial_{\nu_z} u \\ &= \int_S \left[N^\epsilon(x,z) - N(x,z)\right]\partial_{\nu_z} v - \left[N^\epsilon(y,z) - N(y,z)\right]\partial_{\nu_z} u\end{aligned}$$

From the second proof of the fundamental solution, we know that $\Delta N^\epsilon \to \delta$ as $\epsilon \to 0$. Similarly, since $N^\epsilon \to N$ as $\epsilon \to 0$, and the sequence N^ϵ is bounded by $|N|$, the Dominated Convergence theorem tells us that the right hand side integrals go to zero. Thus

$$u * \Delta N^\epsilon(y) - v * \Delta N^\epsilon(x) = \int_S \left[N^\epsilon(x,z) - N(x,z)\right]\partial_{\nu_z} v - \left[N^\epsilon(y,z) - N(y,z)\right]\partial_{\nu_z} u.$$

Sending $\epsilon \to 0$ in this statement gives

$$\begin{aligned} u * \delta(y) - v * \delta(x) &= 0 \\ u(y) - v(z) &= 0 \\ G(x,y) - N(x,y) + N^\epsilon(x,y) - G(y,x) + N(y,x) - N^\epsilon(y,x) &= 0 \\ G(x,y) - G(y,x) = 0 \quad &\Rightarrow \quad G(x,y) = G(y,x)\end{aligned}$$

because N and N^ϵ are radial functions and in either case

$$N(x,y) = N(x-y) = N(y-x) = N(y,x) \qquad N^\epsilon(x,y) = N^\epsilon(y,x)$$

and those terms drop out of the equation. ∎

With this symmetry, we can extend G to a function on $\overline{\Omega} \times \overline{\Omega}$ by setting $G(x, y) = 0 \; \forall \, x \in S$.

Using the Green's function, we want to solve the Dirichlet problem:

$$\Delta u = f \text{ on } \Omega \quad u = 0 \text{ on } S.$$

Setting

$$u(x) = \int_\Omega G(x, y) f(y) \; dy$$

gives a solution because

$$\begin{aligned} u(x) &= \int_\Omega G(x, y) f(y) \; dy \\ &= \int_\Omega N(x, y) f(y) \; dy + \int_\Omega \left[G(x, y) - N(x, y) \right] f(y) \; dy \\ &= f * N(x) + \int_\Omega \left[G(x, y) - N(x, y) \right] f(y) \; dy \\ \Delta u(x) &= f + 0 = f \end{aligned}$$

since N is the fundamental solution and $G(x, y) - N(x, y)$ is harmonic in x. Also, if x is on the boundary, $G(x, y) = 0$, so $u(x) = 0$. So $u(x)$ is the desired solution.

Now, assume we want to solve

$$\Delta w = 0 \text{ on } \Omega \quad w = g \text{ on } S$$

with g continuous on S, and we want w to be continuous on $\overline{\Omega}$. If we assume that $w \in C^1$, then we can use Green's Identity to get that the candidate solution is

$$w(x) = \int_S g(y) \partial_{\nu_y} G(x, y) \; d\sigma(y).$$

Since $\partial_{\nu_y} G(x, y)$ is harmonic in x, it is clear that w is harmonic. It is also claimed that $w = g$ on S. The proof of this statement requires more techniques than will be developed here.

The function $\partial_{\nu_y} G(x, y)$ on $\Omega \times S$ is called the **Poisson Kernel** for Ω, and the above formula gives the **Poisson Integral Formula** for the solution of the Dirichlet problem.

3.5 Examples

In all of these examples, we will be dealing with cases where the dimension of the space is greater than or equal to three. This will allow us to use the form of the fundamental solution (Section 3.3) and Green's function (Section 3.4) that have previously been derived.

3.5.1 Dirichlet Problem in the Half Space

Define the space

$$\mathbb{R}^{n+1}_+ = \{[x,t] \in \mathbb{R}^n \times \mathbb{R} : t > 0\}$$

with $n \geq 2$. This is the half space on which we want to solve the Dirichlet Problem, where the Laplacian is written

$$\Delta = \sum_{i=1}^{n} \frac{\partial^2}{\partial x_i^2} + \frac{\partial^2}{\partial t^2} = \Delta_x + \partial_t^2.$$

In order to define the Green's function, we realize that if we put a point source at $[x,t]$ and one at $[x,-t]$, then the value of the function at $t=0$ will always be zero.

Thus, the Green's function for the half space is

$$G([x,t],[y,s]) = N([x,t],[y,s]) - N([x,-t],[y,s]) = N([x-y,t-s]) - N([x-y,-t-s])$$

where N is the fundamental solution from Section 3.3.

This satisfies the two properties of the Green's function since it goes to zero when s or $t=0$ because N is radial and it satisfies

$$\Delta_{[y,s]} G([x,t],[y,s]) = \delta([x-y,t-s])$$

so $G([x,t],\cdot) - N([x,t],\cdot)$ is harmonic on $\mathbb{R}^{n+1}_+$.

Thus, as discussed in Section 3.4, if we want to solve the Dirichlet Problem

$$\Delta_x u + \partial_t^2 u = f \qquad u([x,0]) = 0$$

we can use the function

$$u([x,t]) = \int_0^\infty \int_{\mathbb{R}^n} G([x,t],[y,s]) f([y,s])\ dy\ ds.$$

If we want to solve the dual Dirichlet Problem,

$$\Delta_x u + \partial_t^2 u = 0 \qquad u([x,0]) = g(x)$$

we need the Poisson kernel. Since the outward normal derivative on the boundary is $-\frac{\partial}{\partial t}$, we can write that

$$-\frac{\partial}{\partial s} G([x,t],[y,s])\bigg|_{s=0} = \frac{2t}{\omega_{n+1}(|x-y|^2+t^2)^{(n+1)/2}}.$$

So, as discussed before, the candidate solution is

$$u([x,t]) = \int_{\mathbb{R}^n} \frac{2t}{\omega_{n+1}(|x-y|^2+t^2)^{(n+1)/2}} g(y)\ dy$$

or, defining

$$P_t(x) = \frac{2t}{\omega_{n+1}(|x|^2 + t^2)^{(n+1)/2}},$$

this solution is $g * P_t(x)$, with the convolution over $\mathbb{R}^n$.

We want to verify that this solution goes to g on the boundary $t = 0$. A key observation shows that

$$P_t(x) = t^{-n} P_1(t^{-1}x)$$

Then, using Theorem 3.2, if $g \in L^p$, we only need to show that $\int P_1 = 1$ for $g * P_t(x) \to g$ as $t \to 0$.

$$\begin{aligned}
\int P_1(x)\, dx &= \int \frac{2}{\omega_{n+1}(|x|^2+1)^{(n+1)/2}}\, dx \\
&= \frac{2\omega_n}{\omega_{n+1}} \int_0^\infty \frac{r^{n-1}\, dr}{(r^2+1)^{(n+1)/2}} \\
&= \frac{\Gamma(\frac{1}{2}(n+1))}{\Gamma(\frac{1}{2}n)\Gamma(\frac{1}{2})} \int_0^1 s^{(n/2)-1}(1-s)^{-1/2}\, ds = 1
\end{aligned}$$

by the substitution $s = \frac{r^2}{r^2+1}$ and the formula for the beta integral.

Therefore, we have the desired result that the solution u goes to g on the boundary of the region. However, this solution is not unique, because if u is a solution, then so is $u+ct$. But, if g is bounded and continuous, then $u = g * P_t$ is the only bounded solution. We have thus proved the following theorem.

Theorem 3.11 ([3] 2.45)**.** *If g is continuous and vanishes at infinity on $\mathbb{R}^n$, then $u([x,t]) = g*P_t(x)$ vanishes at infinity on $\overline{\mathbb{R}^{n+1}_+}$, and it is the unique solution of the Dirichlet problem with this property.*

3.5.2 Dirichlet Problem in the Ball

Now, we want to take a unit ball, $B_1(0)$, in $\mathbb{R}^n$, and solve the Dirichlet problem via the Green's function and Poisson kernel. The idea is the same as in the half space, since a unit charge at x can be canceled by a charge at $x/|x|^2$, which is what you get when you reflect x over the sphere. This second charge, however, must have magnitude $|x|^{2-n}$ in order to cancel the first one on the sphere.

Lemma 3.1 ([3] 2.46)**.** *If $x,\ y \in \mathbb{R}^n$, $x \neq 0$, and $|y| = 1$, then*

$$|x - y| = \left||x|^{-1}x - |x|y\right|.$$

Proof. We have

$$\begin{aligned} |x-y|^2 &= |x|^2 - 2x\cdot y + 1 \\ &= \left||x|y\right|^2 - 2(|x|^{-1}x)\cdot(|x|y) + \left||x|^{-1}x\right|^2 \\ &= \left||x|y - |x|^{-1}x\right|^2. \end{aligned}$$

■

For the case $n > 2$, we define

$$\begin{aligned} G(x,y) &= N(x,y) - |x|^{2-n}N(|x|^{-2}x, y) \\ &= \frac{1}{(2-n)\omega_n}\left[|x-y|^{2-n} - \left||x|^{-1}x - |x|y\right|^{2-n}\right]. \end{aligned}$$

In looking at the first equation, we can see that $G(x,y) - N(x,y)$ is harmonic if

$$\Delta N(|x|^{-2}x, y) = 0 \quad \Leftrightarrow \quad y \neq |x|^{-2}x$$

However, $\left||x|^{-2}x\right| = |x|^{-1}$, so if $x \in B_1(0)$, $|x| < 1$ and $|x|^{-1} > 1$. If $y = |x|^{-2}x$ and $x \in B_1(0)$, then $|y| > 1$, so $y \notin B_1(0)$. Therefore, $G(x,y) - N(x,y)$ is harmonic on $B_1(0)$. Also, if $|y| = 1$, the lemma gives us that $G(x,y) = 0$ by the second equation. A direct calculation can also show that $G(x,y) = G(y,x)$.

From the Green's function, we can compute the Poisson kernel for solving the dual Dirichlet problem:

$$P(x,y) = \partial_{\nu_y} G(x,y) \quad x \in B_1(0),\ y \in S_1(0)$$

which can be calculated using $\partial_{\nu_y} = y \cdot \nabla_y$ on $S_1(0)$ as

$$P(x,y) = \frac{-1}{\omega_n}\left[\frac{y\cdot(x-y)}{|x-y|^n} - \frac{|x|y\cdot(|x|^{-1}x - |x|y)}{||x|^{-1}x - |x|y|^n}\right]$$

Using Lemma 3.1, since $|y| = 1$, this simplifies to

$$P(x,y) = \frac{1-|x|^2}{\omega_n |x-y|^n}.$$

As discussed in Section 3.5.1, if we want to solve the Dirichlet problem

$$\Delta u = f \text{ on } B_1(0) \qquad u = 0 \text{ on } S_1(0)$$

we can use the function

$$u(x) = \int_{B_1(0)} G(x,y) f(y)\, dy$$

and if we want to solve the dual problem we need the Poisson kernel.

Theorem 3.12 ([3] 2.48)**.** *If $f \in L^1(S_1(0))$ and P is as computed above, set*

$$u(x) = \int_S P(x,y) f(y)\ d\sigma(y) \qquad (x \in B_1(0)).$$

Then u is harmonic on $B_1(0)$. If f is continuous, u extends continuously to $\overline{B_1(0)}$ and $u = f$ on $S_1(0)$. If $f \in L^p(S)(1 \leq p < \infty)$, then $u_r \to f$ in the L^p norm as $r \to 1$, where $u_r(y) = u(ry),\ y \in S_1(0)$.

Proof. In this proof, in order to simplify notation, define

$$B := B_1(0) \qquad S := S_1(0).$$

For each $x \in B$, $P(x,y)$ is bounded for all y in S, since $|x-y| \neq 0\ \forall\, y \in S$, so the function $u(x)$ is well-defined. Since $G(x,y)$, and therefore $P(x,y)$ is harmonic in x, u is also harmonic.

Claim 1 For any $y_0 \in S$ and any neighborhood V of y_0 in S,

$$\lim_{r\to 1} \int_{S\setminus V} P(ry_0, y)\ d\sigma(y) = 0.$$

Proof.

$$P(ry_0, y) = \frac{1-r^2}{\omega_n |ry_0 - y|^n}$$

The denominator of this function is uniformly bounded away from 0 for $|r| < 1$ and outside of a neighborhood of y_0. Thus, the integral is defined, and the integrand goes to 0 as $r \to 1$. ■

Claim 2 $\int_S P(x,y)\ d\sigma(y) = 1\ \forall\, x \in B$.

Proof. Since P is harmonic in x, we can use the mean value property around 0 to get that

$$\omega_n P(0,y) = \int_S P(ry', y) d\sigma(y')$$

for any $r \in (0,1)$, which defines a sphere around the origin. However,

$$P(0,y) = \frac{1-0}{\omega_n |0-y|^n} = \frac{1}{\omega_n}\ \forall\, y \in S$$

and the lemma above gives that $P(ry', y) = P(ry, y')$. Setting $x = ry \in B$ gives

$$1 = \omega_n \frac{1}{\omega_n} = \int_S P(x, y')\ d\sigma(y'). \qquad ■$$

Suppose that f is continuous on S, which means it is uniformly continuous. Given $\epsilon > 0$, choose $\delta > 0$ such that $|x - y| < \delta \Rightarrow |f(x) - f(y)| < \frac{\epsilon}{2}$. Define $V_x = \{y \in S : |x - y| < \delta \}$. Then, for any $x \in S$, $r < 1$

$$\begin{aligned} |f(x) - u(rx)| &= \left| \int_S [f(x) - f(y)] P(rx, y) \, d\sigma(y) \right| \\ &\leq \sup_{y \in V_x} \{|f(x) - f(y)|\} \int_{V_x} P(rx, y) \, d\sigma(y) + 2 \sup_{x \in S \setminus V_x} \{|f(x)|\} \int_{S \setminus V_x} P(rx, y) \, d\sigma(y) \end{aligned}$$

The first term is less than $\frac{\epsilon}{2}$, since we are on V_x and the integral is less than 1 by claim 2. Similarly, there is an δ' such that if $1 - r < \delta'$, then the value of the integral in the second term is less than $\frac{\epsilon}{4||f||_\infty}$. Therefore, this sum is less than ϵ, and $u_r \to f$ as $r \to 1$, and u extends continuously to $\overline{B}$ with $u = f$ on S.

Finally, suppose $f \in L^p$. Given $\epsilon > 0$, choose $g \in C(S)$ with $||g - f||_p \leq \frac{\epsilon}{3}$, which exists because $C(S)$ is dense in L^p. Setting $v(x) = \int_{S_1(0)} P(x, y) g(y) \, d\sigma(y)$, we have

$$||f - u_r||_p \leq ||f - g||_p + ||g - v_r||_p + ||v_r - u_r||_p.$$

The first term on the right is less than $\frac{\epsilon}{3}$ by definition, and the second term is also less than $\frac{\epsilon}{3}$ if $1 - r$ is small enough. The third term can be shown to be smaller than $\frac{\epsilon}{3}$ by the generalized Young's Inequality, (Theorem 3.1) in [3], since P is a positive function with integral 1 on S, and $||f - g||_p \leq \frac{\epsilon}{3}$. Therefore, this sum is less than ϵ, and $u_r \to f$ in the L^p norm as $r \to 1$.

■

4 Inverse Problem

The forward problem is a deterministic differential equation that can be solved numerically. The inverse problem, however, requires a different approach. In engineering applications, it is assumed that we will be able to measure temperature and an input flux, but we do not know what the inside of the material looks like. In this specific case, we are looking at a defined rectangle Ω, and it is assumed that we know the thermal properties α_i and k_i for each region. We are trying to determine which portion of the plate has been corroded. In mathematical terms, we are attempting to find the boundary of the two domains Ω_1 and Ω_2. In deriving a solution, it is assumed that this curve is a function of horizontal position, $C(x)$, that is supported away from the edges of the plate. Assuming that the second region is corroded or missing material, knowing this function $C(x)$ could help determine the safety of that component in the structure or if it needs to be replaced.

Intuition says that the change in material properties should affect the way the heat flows through the object. We hope that this will cause a significant change in the temperature profile of the plate, specifically on the top surface. Figure 4.1 shows a COMSOL image of the temperature in two identical plates after a given amount of time. The only difference between the two plates is the missing material at the bottom of the left plate.

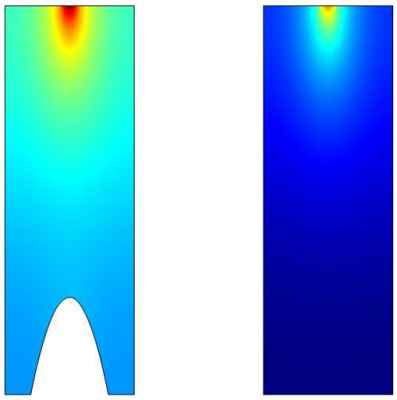

Figure 4.1: COMSOL Images Showing Changes in Temperature Profile Due to Corrosion

As can be seen in the figure above, there is clearly a difference in the temperature at the top of the plate caused by the missing material at the bottom. This gives us hope that we should be able to recover at least some information about the corrosion profile from the accessible surface temperature.

This work on the inverse problem was conducted with partner Andrew Rzeznik (Cornell University) at the NSF-REU at Rose-Hulman Institute of Technology, under the guidance of Dr. Kurt Bryan. What follows is the majority of the results paper from our summer research. The full paper has been submitted to SIURO for publication and is currently in revision [5].

5 Solving the Inverse Problem

The approach to solving this inverse problem involves applying Green's Identity and a linearization approximation to the heat equation to generate a simplified set of equations that can be solved numerically. The layout of the problem can be seen in Section 2, with the equations as stated there. The goal is to find the curve $C(x)$ given data for u_1 along the top surface $y = 1$.

5.1 Computations

In order to solve this inverse problem, we employed the so-called "Reciprocity Gap" approach, which is an application of Green's Identities to this specific problem. The idea is to extract information about the function $C(x)$ from boundary data by integrating u by parts against strategically chosen test functions. We begin with

Theorem 5.1 (Green's Second Identity)**.** *For any bounded region $D \subset \mathbb{R}^2$ with piecewise smooth boundary ∂D, and any two functions $u, v \in C^2(\overline{D})$, we have*

$$\int_D (u\Delta v - v\Delta u)\ dA = \int_{\partial D} \left(u\frac{\partial v}{\partial \vec{n}} - v\frac{\partial u}{\partial \vec{n}} \right)\ ds.$$

We want to use Green's Identity, combined with what we know about both the interior and the boundary of Ω, in order to generate an approximation for the function $C(x)$.

In what follows we will use a collection of "test functions" ϕ_k, $1 \leq k \leq M$, for some M. The higher M is, the more test functions are being used in the construction, and the more accurately the corrosion profile can be determined. Each test function ϕ_k will satisfy (see Section 5.2.1 for the construction of specific ϕ_k)

$$\begin{aligned} \frac{\partial \phi}{\partial t} + \alpha_1 \Delta \phi &= 0 \text{ on } \Omega \\ \frac{\partial \phi}{\partial \vec{n}} &= 0 \text{ on } y = 0,\ x = 0, \text{ and } x = L \\ \phi(x, y, T) &= 0 \text{ on } \Omega. \end{aligned}$$

We start with the equation

$$\int_0^T \int_{\Omega_1} u_1 \left(\frac{\partial \phi}{\partial t} + \alpha_1 \Delta \phi \right)\ dA\ dt = 0$$

or

$$\int_0^T \int_{\Omega_1} u_1 \frac{\partial \phi}{\partial t}\ dA\ dt + \alpha_1 \int_0^T \int_{\Omega_1} u_1 \Delta \phi\ dA\ dt = 0.$$

Integrating the first term by parts in time and using Green's Identity on the second term gives

$$\int_{\Omega_1} \left(u_1 \phi|_0^T - \int_0^T \phi \frac{\partial u_1}{\partial t}\ dt \right)\ dA + \alpha_1 \int_0^T \left(\int_{\Omega_1} \phi \Delta u_1\ dA + \int_{\partial \Omega_1} \left(u_1 \frac{\partial \phi}{\partial \vec{n}} - \phi \frac{\partial u_1}{\partial \vec{n}} \right)\ ds \right) dt = 0$$

or

$$\int_{\Omega_1} u_1\phi|_0^T \; dA - \int_{\Omega_1}\int_0^T \phi\left(\frac{\partial u_1}{\partial t} - \alpha_1\Delta u_1\right)\; dt\; dA + \alpha_1\int_0^T\int_{\partial\Omega_1}\left(u_1\frac{\partial\phi}{\partial\vec{n}} - \phi\frac{\partial u_1}{\partial\vec{n}}\right)\; ds\; dt \;\; = \;\; 0.$$

The first two terms in the above expression are zero because u_1 solves the heat equation and vanishes at $t = 0$, while ϕ vanishes at $t = T$. Canceling the α_1 gives:

$$\int_0^T\int_{\partial\Omega_1}\left(u_1\frac{\partial\phi}{\partial\vec{n}} - \phi\frac{\partial u_1}{\partial\vec{n}}\right)\; ds\; dt = 0$$

or, factoring in the boundary of Ω_1 and the conditions on the functions there,

$$\int_0^T\int_{top}\left(u_1\frac{\partial\phi}{\partial\vec{n}} - \phi\frac{\partial u_1}{\partial\vec{n}}\right)\; ds\; dt + \int_0^T\int_{C(x)}\left(u_1\frac{\partial\phi}{\partial\vec{n}} - \phi\frac{\partial u_1}{\partial\vec{n}}\right)\; ds\; dt = 0 \tag{5.1}$$

where $C(x)$ is defined with the downward normal.

Similarly, we can look at the region Ω_2 and start with

$$\int_0^T\int_{\Omega_2} u_2\frac{\partial\phi}{\partial t}\; dA\; dt + \alpha_1\int_0^T\int_{\Omega_2} u_2\Delta\phi\; dA\; dt \;\; = \;\; 0.$$

Integrating the first term by parts in time and using Green's Identity on the second term gives

$$\int_{\Omega_2}\left(u_2\phi|_0^T - \int_0^T \phi\frac{\partial u_2}{\partial t}\; dt\right)\; dA + \alpha_1\int_0^T\left(\int_{\Omega_2}\phi\Delta u_2\; dA + \int_{\partial\Omega_2}\left(u_2\frac{\partial\phi}{\partial\vec{n}} - \phi\frac{\partial u_2}{\partial\vec{n}}\right)\; ds\right)\; dt = 0.$$

The first term is zero because ϕ and u_2 vanish at the endpoints in time. Since u_2 solves the heat equation in Ω_2, we assume that

$$\frac{\partial u_2}{\partial t} = \alpha_2\Delta u_2.$$

Plugging this in above gives

$$\begin{aligned}
-\alpha_2\int_{\Omega_2}\int_0^T \phi\Delta u_2\; dt\; dA + \alpha_1\int_0^T\int_{\Omega_2}\phi\Delta u_2\; dA\; dt + \alpha_1\int_0^T\int_{\partial\Omega_2}\left(u_2\frac{\partial\phi}{\partial\vec{n}} - \phi\frac{\partial u_2}{\partial\vec{n}}\right)\; ds\; dt &\;\; = \;\; 0\\
(\alpha_1 - \alpha_2)\int_0^T\int_{\Omega_2}\phi\Delta u_2\; dA\; dt + \alpha_1\int_0^T\int_{\partial\Omega_2}\left(u_2\frac{\partial\phi}{\partial\vec{n}} - \phi\frac{\partial u_2}{\partial\vec{n}}\right)\; ds\; dt &\;\; = \;\; 0\\
\frac{\alpha_1 - \alpha_2}{\alpha_1}\int_0^T\int_{\Omega_2}\phi\Delta u_2\; dA\; dt + \int_0^T\int_{\partial\Omega_2}\left(u_2\frac{\partial\phi}{\partial\vec{n}} - \phi\frac{\partial u_2}{\partial\vec{n}}\right)\; ds\; dt &\;\; = \;\; 0.
\end{aligned}$$

Taking the boundary of Ω_2 into consideration gives

$$\frac{\alpha_1 - \alpha_2}{\alpha_1}\int_0^T\int_{\Omega_2}\phi\Delta u_2\; dA\, dt + \int_0^T\int_{C(x)}\left(u_2\frac{\partial\phi}{\partial\vec{n}} - \phi\frac{\partial u_2}{\partial\vec{n}}\right)\; ds\, dt + \int_0^T\int_{bottom}\left(u_2\frac{\partial\phi}{\partial\vec{n}} - \phi\frac{\partial u_2}{\partial\vec{n}}\right)\; ds\, dt = 0,$$

where $C(x)$ has the upward normal. Flipping the normal on $C(x)$ so it can be combined with equation (5.1) and canceling the last term since both functions have zero normal derivative at $y = 0$ gives

$$\frac{\alpha_1 - \alpha_2}{\alpha_1} \int_0^T \int_{\Omega_2} \phi \Delta u_2 \; dA \; dt - \int_0^T \int_{C(x)} \left(u_2 \frac{\partial \phi}{\partial \vec{n}} - \phi \frac{\partial u_2}{\partial \vec{n}} \right) \; ds \; dt = 0 \tag{5.2}$$

where $C(x)$ is defined with the downward normal.

We now seek to combine equations (5.1) and (5.2) to generate a relation that will allow us to approximate the function $C(x)$. We will use the temperature profile u_2 in Ω_2 and the continuity conditions on $C(x)$ to do this.

5.2 Combining Equations

To start, modify equation (5.1) using the continuity conditions on $C(x)$, to give

$$\int_0^T \int_{top} \left(u_1 \frac{\partial \phi}{\partial \vec{n}} - \phi \frac{\partial u_1}{\partial \vec{n}} \right) \; ds \; dt + \int_0^T \int_{C(x)} \left(u_2 \frac{\partial \phi}{\partial \vec{n}} - \frac{k_2}{k_1} \phi \frac{\partial u_2}{\partial \vec{n}} \right) \; ds \; dt = 0. \tag{5.3}$$

Then, adding equations (5.2) and (5.3) gives:

$$\int_0^T \int_{top} \left(u_1 \frac{\partial \phi}{\partial \vec{n}} - \phi \frac{\partial u_1}{\partial \vec{n}} \right) \; ds \; dt + \left(1 - \frac{k_2}{k_1} \right) \int_0^T \int_{C(x)} \phi \frac{\partial u_2}{\partial \vec{n}} \; ds \; dt + \frac{\alpha_1 - \alpha_2}{\alpha_1} \int_0^T \int_{\Omega_2} \phi \Delta u_2 \; dA \; dt = 0.$$

Defining

$$RG(\phi) = \int_0^T \int_{top} \left(u_1 \frac{\partial \phi}{\partial \vec{n}} - \phi \frac{\partial u_1}{\partial \vec{n}} \right) \; ds \; dt \tag{5.4}$$

and rearranging gives

$$RG(\phi) = \left(\frac{k_2}{k_1} - 1 \right) \int_0^T \int_{C(x)} \phi \frac{\partial u_2}{\partial \vec{n}} \; ds \; dt + \frac{\alpha_2 - \alpha_1}{\alpha_1} \int_0^T \int_{\Omega_2} \phi \Delta u_2 \; dA \; dt.$$

Knowing that u_2 solves the heat equation on Ω_2 and that on $C(x)$

$$\vec{n} = \frac{< C'(x), -1 >}{\sqrt{C'(x)^2 + 1}} \qquad \text{and} \qquad ds = \sqrt{C'(x)^2 + 1},$$

this expression can be written as

$$RG(\phi) = \left(\frac{k_2}{k_1} - 1 \right) \int_0^T \int_0^L C'(x) \phi \frac{\partial u_2}{\partial x} \bigg|_{C(x)} - \phi \frac{\partial u_2}{\partial y} \bigg|_{C(x)} dx \; dt + \frac{\alpha_2 - \alpha_1}{\alpha_1 \alpha_2} \int_0^T \int_{\Omega_2} \phi \frac{\partial u_2}{\partial t} \; dA \; dt \tag{5.5}$$

which is the fully simplified non-linear problem.

5.2.1 Generation of Test Functions

We want to numerically generate test functions ϕ_k such that

$$\begin{aligned} \frac{\partial \phi_k}{\partial t} + \alpha_1 \Delta \phi_k &= 0 \text{ on } \Omega \\ \frac{\partial \phi_k}{\partial \vec{n}} &= 0 \text{ on } y = 0,\ x = 0, \text{ and } x = L \\ \phi_k(x, y, T) &= 0 \text{ on } \Omega \end{aligned}$$

In order to do this, we look for a related function ψ_k, which satisfies

$$\begin{aligned} \frac{\partial \psi_k}{\partial t} - \alpha_1 \Delta \psi_k &= 0 \text{ on } \Omega \\ \frac{\partial \psi_k}{\partial \vec{n}} &= 0 \text{ on } y = 0,\ x = 0, \text{ and } x = L \\ \psi_k(x, y, 0) &= 0 \text{ on } \Omega \end{aligned}$$

Then, letting $\phi_k(x, y, t) = \psi_k(x, y, T - t)$ will give the desired functions ϕ_k. In order to find ψ, we will utilize the Green's Function for heat, and model a situation with point heat sources.

The Green's Function for heat is

$$K_{(x_0,y_0)}(x, y, t) = \frac{1}{4\pi\alpha t} e^{-\frac{(x-x_0)^2+(y-y_0)^2}{4\alpha t}}$$

which satisfies

$$\begin{aligned} \frac{\partial K}{\partial t} - \alpha \Delta K &= 0 \text{ on } \mathbb{R}^2 \\ K(x, y, 0) &= \delta(x - x_0, y - y_0) \end{aligned}$$

where δ is the Kronecker delta function. This function models the spread of a point impulse heat source at the point (x_0, y_0).

By Duhamel's Principle, and by carrying out the calculations, it can be shown that

$$\int_0^t K_{(x_0,y_0)}(x, y, \tau)\ d\tau$$

is also a solution to the heat equation with zero initial condition. It models the spread of a constant heat source at the point (x_0, y_0). Since the initial condition is zero, any sum of these integrals will also solve the heat equation with zero initial condition.

In order to specify the zero Neumann data conditions for ψ, we need to use the method of images. The idea is if we make the array of point sources symmetric around some line, then heat has no reason to flow across the line, resulting in zero normal derivative on that line. Take an initial

point (x_0, y_0), and reflect it over $x = 0$ to get $(x_0, -y_0)$. These two point sources together form a temperature profile with zero Neumann data at $x = 0$. Since we also want zero Neumann Data at $x = L$, we reflect these two points over that line, but to maintain symmetry about $x = 0$, we also reflect over $x = -L$. Repeating this process gives a set of points of the form $(x_0, 2jL - y_0)$ and $(x_0, 2jL + y_0)$ for $j \in \{-N, ..., N\}$. This is demonstrated in Figure 5.1 below.

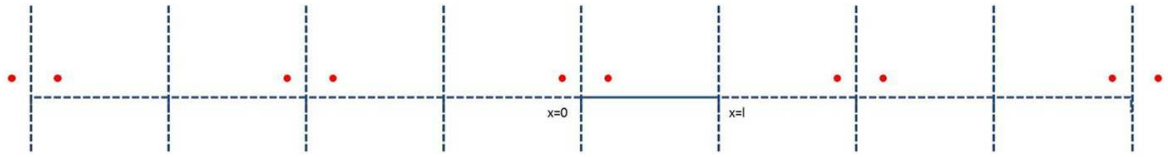

Figure 5.1: Set of Reflections in the X-Direction for the Method of Images

This set of points is not completely symmetric about the line $x = L$, but the variance from symmetry is 4 point sources more than NL units away. Since the heat equation drops off as distance squared, these points have almost no effect on the heat flux at $x = L$, so we can take that flux to be approximately zero. The equation describing the temperature profile in this situation is

$$\sum_{j=-N}^{N} \int_0^t K_{(2jl+x_0,y_0)}(x, y, \tau) + K_{(2jl-x_0,y_0)}(x, y, \tau)\ d\tau.$$

Finally, to ensure zero Neumann data at $y = 0$, we reflect all of these points over the line $y = 0$, giving a diagram similar to that in Figure 5.2 below.

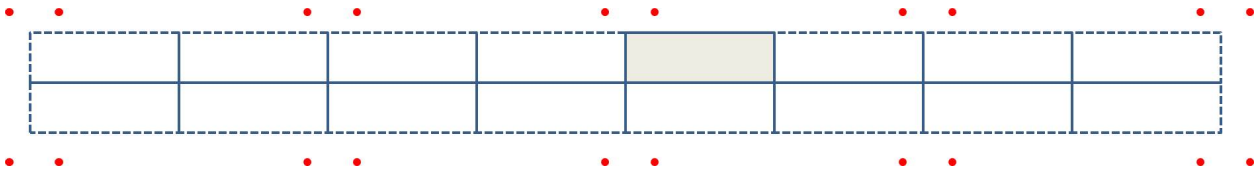

Figure 5.2: Full Set of Reflections for the Method of Images

The equation describing the temperature profile given these point sources, which satisfies the heat equation, zero initial conditions, and the desired Neumann boundary conditions is

$$\psi(x, y, t) = \sum_{j=-N}^{N} \int_0^t \Big[K_{(2jl+x_0,y_0)}(x, y, \tau) + K_{(2jl-x_0,y_0)}(x, y, \tau) + K_{(2jl+x_0,-y_0)}(x, y, \tau) + K_{(2jl-x_0,-y_0)}(x, y, \tau)\Big]\ d\tau.$$

Defining $\phi(x, y, t) = \psi(x, y, T-t)$ satisfies all the desired conditions. The necessary derivatives were computed analytically and then used in the MATLAB code to create the numerical ϕ functions. In order to generate the set of functions used in the calculations, we defined the set of points for the

first heat source, $(x_0, y_0)_k$ where $x_0 \in \{1, ..., 9\}$ and $y_0 \in \{1.1, ..., 1.5\}$. Working out the derivatives for ϕ gives:

$$\phi = \int_0^{T-t} \frac{1}{4\pi\alpha\tau}\left(e^{-\frac{(y-y_0)^2}{4\alpha\tau}} + e^{-\frac{(y+y_0)^2}{4\alpha\tau}}\right)\sum_{j=-N}^{N}\left(e^{-\frac{(x-(2jL+x_0))^2}{4\alpha\tau}} + e^{-\frac{(x-(2jL-x_0))^2}{4\alpha\tau}}\right)d\tau$$

$$\left.\frac{\partial\phi}{\partial t}\right|_{y=0} = \frac{-1}{2\pi\alpha(T-t)}e^{\frac{-y_0^2}{4\alpha(T-t)}}\sum_{j=-N}^{N}\left(e^{-\frac{(x-(2jL+x_0))^2}{4\alpha(T-t)}} + e^{-\frac{(x-(2jL-x_0))^2}{4\alpha(T-t)}}\right)$$

$$\left.\frac{\partial\phi}{\partial x}\right|_{y=0} = \frac{-e^{\frac{-y_0^2}{4\alpha(T-t)}}}{\pi\alpha}\sum_{j=-N}^{N}\left(\frac{x-(2jL+x_0)}{(x-(2jL+x_0))^2+y_0^2}e^{-\frac{(x-(2jL+x_0))^2}{4\alpha(T-t)}} + \frac{x-(2jL-x_0)}{(x-(2jL-x_0))^2+y_0^2}e^{-\frac{(x-(2jL-x_0))^2}{4\alpha(T-t)}}\right)$$

$$\left.\frac{\partial\phi}{\partial y}\right|_{y=1} = \frac{-1}{2\pi\alpha}\sum_{j=-N}^{N}\Bigg[(1-y_0)e^{-\frac{(1-y_0)^2}{4\alpha(T-t)}}\left(\frac{e^{-\frac{(x-(2jL+x_0))^2}{4\alpha(T-t)}}}{(x-(2kL+x_0))^2+(1-y_0)^2} + \frac{e^{-\frac{(x-(2jL-x_0))^2}{4\alpha(T-t)}}}{(x-(2kL-x_0))^2+(1-y_0)^2}\right)$$
$$+(1+y_0)e^{-\frac{(1+y_0)^2}{4\alpha(T-t)}}\left(\frac{e^{-\frac{(x-(2jL+x_0))^2}{4\alpha(T-t)}}}{(x-(2kL+x_0))^2+(1+y_0)^2} + \frac{e^{-\frac{(x-(2jL-x_0))^2}{4\alpha(T-t)}}}{(x-(2kL-x_0))^2+(1+y_0)^2}\right)\Bigg]$$

5.3 Linearization

The next step to approximating the solution to this inverse problem is linearization. Specifically, we assume that the corrosion profile is a small perturbation of the uncorroded back surface $y = 0$, and then use this assumption to formally linearize the relationship between the function $C(x)$ and the top surface temperature data. Unlike in the electrical case (see [1]) where there is only one differential equation to solve (Laplace's equation), there are two distinct heat equations in Ω_1 and Ω_2 because of the different thermal diffusivities, and this slightly complicates the procedure. For this procedure, we focus on the heat equation in Ω_1 and allow the linearization assumption to take care of the terms from Ω_2.

Making the linearization assumption as stated above, we assume that

$$C(x) = \epsilon C_0(x)$$

or that the corrosion profile is very small.

The last term in equation (5.5) may be written as

$$\frac{\alpha_2 - \alpha_1}{\alpha_1\alpha_2}\int_0^T\int_0^L\int_0^{C(x)}\phi\frac{\partial u_2}{\partial t}\,dy\,dx\,dt.$$

If $C(x)$ is small, we can approximate the function $\phi\frac{\partial u_2}{\partial t}$ by a constant over the innermost integral in y. This term can then be written as approximately equal to

$$\frac{\alpha_2 - \alpha_1}{\alpha_1\alpha_2}\int_0^T\int_0^L C(x)\,\phi\frac{\partial u_2}{\partial t}\bigg|_{y=0}dx\,dt$$

where we choose to evaluate the functions at $y = 0$.

We also want to linearize the parts of the first integral in equation (5.5) about the line $y = 0$, ignoring all terms of $O(\epsilon^2)$.

$$\begin{aligned}
C'(x)\ \phi\frac{\partial u_2}{\partial x}\bigg|_{C(x)} &= C'(x)\ \phi\frac{\partial u_2}{\partial x}\bigg|_{y=0} + C(x)C'(x)\ \frac{\partial \phi}{\partial y}\frac{\partial u_2}{\partial x}\bigg|_{y=0} + C(x)C'(x)\ \phi\frac{\partial^2 u_2}{\partial x \partial y}\bigg|_{y=0} \\
&= C'(x)\ \phi\frac{\partial u_2}{\partial x}\bigg|_{y=0} + O(\epsilon^2) \\
\phi\frac{\partial u_2}{\partial y}\bigg|_{C(x)} &= \phi\frac{\partial u_2}{\partial y}\bigg|_{y=0} + C(x)\ \frac{\partial \phi}{\partial y}\frac{\partial u_2}{\partial y}\bigg|_{y=0} + C(x)\ \phi\frac{\partial^2 u_2}{\partial y^2}\bigg|_{y=0} + O(\epsilon^2) \\
&= 0 + 0 + C(x)\ \phi\frac{\partial^2 u_2}{\partial y^2}\bigg|_{y=0} + O(\epsilon^2).
\end{aligned}$$

Using RG to also refer to the linearized version of (5.5) and plugging the linearized terms in gives

$$RG(\phi) = \left(\frac{k_2}{k_1} - 1\right)\int_0^T\int_0^L \left(C'(x)\ \phi\frac{\partial u_2}{\partial x}\bigg|_{y=0} - C(x)\ \phi\frac{\partial^2 u_2}{\partial y^2}\bigg|_{y=0} dx\right) dt + \frac{\alpha_2 - \alpha_1}{\alpha_1\alpha_2}\int_0^T\int_0^L C(x)\ \phi\frac{\partial u_2}{\partial t}\bigg|_{y=0} dx\, dt. \tag{5.6}$$

Integrating the first term in equation (5.6) by parts in x (integrating $C'(x)$) and rearranging terms gives

$$\begin{aligned}
RG(\phi) &= \left(\frac{k_2}{k_1} - 1\right)\int_0^T \Bigg(C(x)\phi\frac{\partial u_2}{\partial x}\bigg|_{x=0}^{x=L} + \Bigg[\int_0^L -C(x)\ \frac{\partial \phi}{\partial x}\frac{\partial u_2}{\partial x}\bigg|_{y=0} - C(x)\ \phi\frac{\partial^2 u_2}{\partial x^2}\bigg|_{y=0} \\
&\quad -C(x)\ \phi\frac{\partial^2 u_2}{\partial y^2}\bigg|_{y=0} dx\Bigg]\Bigg) dt + \frac{\alpha_2 - \alpha_1}{\alpha_1\alpha_2}\int_0^T\int_0^L C(x)\ \phi\frac{\partial u_2}{\partial t}\bigg|_{y=0} dx\ dt
\end{aligned}$$

where the first term is zero because $\frac{\partial u_2}{\partial x} = 0$ at both sides of the rectangle. Combining the two second derivatives into a Laplacian and separating the first term of the integral gives

$$\begin{aligned}
RG(\phi) &= \left(\frac{k_2}{k_1} - 1\right)\int_0^T\int_0^L -C(x)\ \frac{\partial \phi}{\partial x}\frac{\partial u_2}{\partial x}\bigg|_{y=0} dx\ dt - \left(\frac{k_2}{k_1} - 1\right)\int_0^T\int_0^L C(x)\ \phi\Delta u_2|_{y=0}\ dx\ dt \\
&\quad + \frac{\alpha_2 - \alpha_1}{\alpha_1\alpha_2}\int_0^T\int_0^L C(x)\ \phi\frac{\partial u_2}{\partial t}\bigg|_{y=0} dx\ dt.
\end{aligned}$$

Converting the second term to a time derivative by the heat equation and reorganizing some terms gives

$$\begin{aligned}
RG(\phi) &= \left(\frac{k_2}{k_1} - 1\right)\int_0^T\int_0^L -C(x)\ \frac{\partial \phi}{\partial x}\frac{\partial u_2}{\partial x}\bigg|_{y=0} dx\ dt - \left(\frac{k_2}{k_1} - 1\right)\int_0^T\int_0^L C(x)\ \frac{\phi}{\alpha_2}\frac{\partial u_2}{\partial t}\bigg|_{y=0} dx\ dt \\
&\quad + \frac{\alpha_2 - \alpha_1}{\alpha_1}\int_0^T\int_0^L C(x)\ \frac{\phi}{\alpha_2}\frac{\partial u_2}{\partial t}\bigg|_{y=0} dx\ dt
\end{aligned}$$

or

$$RG(\phi) = \left(\frac{k_2}{k_1} - 1\right) \int_0^T \int_0^L -C(x) \left. \frac{\partial \phi}{\partial x} \frac{\partial u_2}{\partial x} \right|_{y=0} dx\, dt - \left[\left(\frac{k_2}{k_1} - 1\right) - \frac{\alpha_2 - \alpha_1}{\alpha_1} \right] \int_0^T \int_0^L C(x) \left. \frac{\phi}{\alpha_2} \frac{\partial u_2}{\partial t} \right|_{y=0} dx\, dt.$$

Simplifying the coefficient of the second term gives

$$\begin{aligned} \left(\frac{k_2}{k_1} - 1\right) - \frac{\alpha_2 - \alpha_1}{\alpha_1} &= \frac{k_2}{k_1} - 1 - \frac{\alpha_2}{\alpha_1} + 1 \\ &= \frac{k_2}{k_1} - \frac{\alpha_1}{\alpha_2} \end{aligned}$$

Thus, our expression becomes

$$RG(\phi) = \left(\frac{k_2}{k_1} - 1\right) \int_0^T \int_0^L -C(x) \left. \frac{\partial \phi}{\partial x} \frac{\partial u_2}{\partial x} \right|_{y=0} dx\, dt - \left(\frac{k_2}{k_1} - \frac{\alpha_2}{\alpha_1}\right) \int_0^T \int_0^L C(x) \left. \frac{\phi}{\alpha_2} \frac{\partial u_2}{\partial t} \right|_{y=0} dx\, dt. \quad (5.7)$$

Now, making the assumption that the temperature profile u_1 is close to the uncorroded temperature profile u_0, which is reasonable in the case that $C(x)$ is small, we get

$$u_1 = u_0 + \epsilon \tilde{u_1}$$

We evaluate this expression on the curve $C(x)$ to obtain

$$u_2|_{C(x)} = u_1|_{C(x)} = u_0|_{C(x)} + \epsilon\, \tilde{u_1}|_{C(x)}\,.$$

Linearizing the far left and far right about $y = 0$ gives

$$u_2|_{y=0} + C(x) \left. \frac{\partial u_2}{\partial y} \right|_{y=0} + O(\epsilon^2) = u_0|_{y=0} + C(x) \left. \frac{\partial u_0}{\partial y} \right|_{y=0} + O(\epsilon^2) + \epsilon\, \tilde{u_1}|_{y=0} + O(\epsilon^2).$$

Since

$$\left. \frac{\partial u_2}{\partial y} \right|_{y=0} = \left. \frac{\partial u_0}{\partial y} \right|_{y=0} = 0$$

we are left with

$$u_2|_{y=0} = u_0|_{y=0} + O(\epsilon).$$

Integrating the last term of equation (5.7) by parts in time will generate a new set of w_k functions which can be used to numerically solve for the function $C(x)$.

$$\begin{aligned} RG(\phi) &= \left(\frac{k_2}{k_1} - 1\right) \int_0^T \int_0^L -C(x) \left. \frac{\partial \phi}{\partial x} \frac{\partial u_0}{\partial x} \right|_{y=0} dx\, dt - \left(\frac{k_2}{k_1} - \frac{\alpha_2}{\alpha_1}\right) \left[u_0 \phi|_0^T - \int_0^T \int_0^L C(x) \left. \frac{u_0}{\alpha_2} \frac{\partial \phi}{\partial t} \right|_{y=0} dx\, dt \right] \\ &= \left(1 - \frac{k_2}{k_1}\right) \int_0^T \int_0^L C(x) \left. \frac{\partial \phi}{\partial x} \frac{\partial u_0}{\partial x} \right|_{y=0} dx\; dt + \left(\frac{k_2}{k_1} - \frac{\alpha_2}{\alpha_1}\right) \int_0^T \int_0^L C(x) \left. \frac{u_0}{\alpha_2} \frac{\partial \phi}{\partial t} \right|_{y=0} dx\; dt \\ &= \int_0^L C(x) \left[\int_0^T \left(1 - \frac{k_2}{k_1}\right) \left. \frac{\partial \phi}{\partial x} \frac{\partial u_0}{\partial x} \right|_{y=0} + \left(\frac{k_2}{k_1} - \frac{\alpha_2}{\alpha_1}\right) \left. \frac{u_0}{\alpha_2} \frac{\partial \phi}{\partial t} \right|_{y=0} dt \right] dx \end{aligned}$$

and, defining

$$w_k(x) := \int_0^T \left(1 - \frac{k_2}{k_1}\right) \frac{\partial \phi_k}{\partial x} \frac{\partial u_0}{\partial x}\bigg|_{y=0} + \left(\frac{k_2}{k_1} - \frac{\alpha_2}{\alpha_1}\right) \frac{u_0}{\alpha_2} \frac{\partial \phi_k}{\partial t}\bigg|_{y=0} dt$$

we are looking for solutions to the system of integral equations,

$$RG(\phi_k) = \int_0^L C(x) w_k(x) dx \tag{5.8}$$

with $1 \leq k \leq M$.

From equation (5.8), we can see that plugging in $C(x) = 0$ gives

$$RG_0(\phi_k) = \int_0^T \int_{top} u_0 \frac{\partial \phi_k}{\partial \vec{n}} - \phi_k \frac{\partial u_0}{\partial \vec{n}} \; ds \; dt = 0. \tag{5.9}$$

Subtracting equation (5.9) from (5.4) gives

$$\tilde{RG}(\phi_k) = \int_0^T \int_{top} \tilde{u_1} \frac{\partial \phi}{\partial \vec{n}} \; ds \; dt = \int_0^L C(x) w_k(x) \; dx \tag{5.10}$$

since

$$\frac{\partial u_0}{\partial \vec{n}}\bigg|_{y=1} = \frac{\partial u_1}{\partial \vec{n}}\bigg|_{y=1}$$

where $\tilde{u_1} = u_1 - u_0$ is the disturbance from the uncorroded temperature profile. This is the expression used to compute the function $C(x)$ in the MATLAB code.

5.4 Finding $C(x)$: Least 2-Norm

From the previous section, we are looking for a solution to the system of equations

$$RG_k = \int_0^L C(x) w_k(x) \; dx \tag{5.11}$$

for $1 \leq k \leq M$. In order to specify a single solution, we look for the function $C(x)$ with the smallest L^2 norm. As shown in [1], the approximation for the function $C(x)$ with this property must be a linear combination of the w_k functions, or

$$C(x) = \sum_{i=1}^{M} \lambda_i w_i(x).$$

Plugging this into equation (5.11) gives

$$\begin{aligned} RG_k &= \int_0^L \sum_{i=1}^{M} \lambda_i w_i(x) w_k(x) \; dx \\ &= \sum_{i=1}^{M} \lambda_i \int_0^L w_i(x) w_k(x) \; dx. \end{aligned}$$

Defining the coefficient matrix $\mathbf{B}$ by

$$\mathbf{B}_{ik} = \int_0^L w_i(x) w_k(x)\ dx$$

gives

$$RG_k = \sum_{i=1}^{N} \mathbf{B}_{ik} \lambda_i$$

for $1 \leq k \leq M$, or

$$\vec{RG} = \mathbf{B}\vec{\lambda}.$$

Then calculating λ via $\mathbf{B}^{-1}\vec{RG}$ and letting

$$C(x) = \sum_{i=1}^{M} \lambda_i w_i(x)$$

gives an approximation for the corrosion profile in the system.

6 Refining the Solution

Performing the procedure in Section 5.4 and using it to approximate the function $C(x)$ gives a graph similar to that in Figure 6.1.

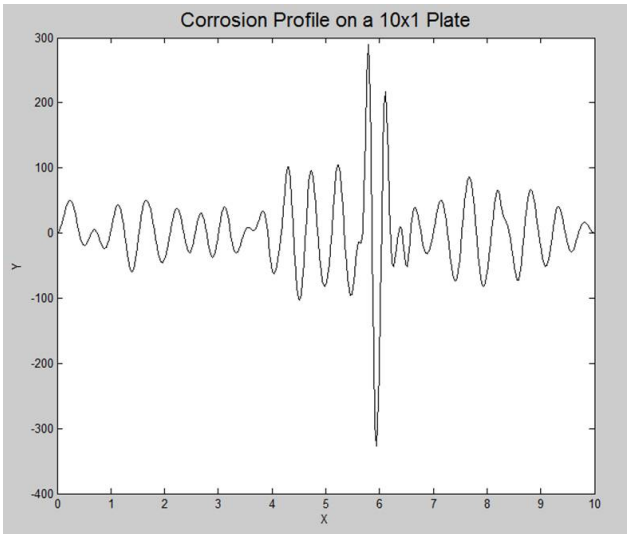

Figure 6.1: Graph of the Raw Approximation of $C(x)$

Since our plate is only supposed to be of thickness 1, this is not a feasible result. We need some way to refine our solution to get something that more closely matches the curve $C(x)$.

6.1 Regularization

The high amplitude values and oscillatory nature of the approximation of $C(x)$ in Figure 6.1 suggest that this inverse problem is ill-posed. In our case, this presents itself in the fact that the matrix $\mathbf{B}$ is ill-conditioned: it has singular values that are very close to zero. Following the analysis in [1], we implemented a regularization process using the singular value decomposition of the matrix $\mathbf{B}$.

We define ϵ_∞ as the maximum absolute error in the system and ϵ_{thresh} as the relative noise on a 0 to 1 scale. These two parameters can be changed to adjust the amount of regularization applied to the system. We then set

$$\epsilon_d = \frac{\sqrt{M} h_w C_{max} \epsilon_\infty}{\epsilon_{thresh}}$$

where M is the number of test functions used, h_w is the average maximum value of the w_k functions, and

$$C_{max} = \max_k \int_0^L \int_0^T \left| \frac{\partial \phi_k}{\partial y} \right| \, dt \, dx.$$

With this ϵ_d defined, we now look at the Singular Value Decomposition of $\mathbf{B}$. If any of the singular values are less than ϵ_d, we set the corresponding value in $\mathbf{B}^{-1}$ to zero, eliminating the high magnitude terms in $\mathbf{B}^{-1}$. Computing the corrosion profile with this modified $\mathbf{B}^{-1}$ matrix gives much better results for the corrosion profile. Figure 6.2 shows how the process of regularization changes the approximation for the curve $C(x)$ for different values of ϵ_∞. In this figure, the solid line shows the reconstructed profile after the stated amount of regularization, and the dashed line is the actual corrosion profile that was used to generate the data used for RG_k.

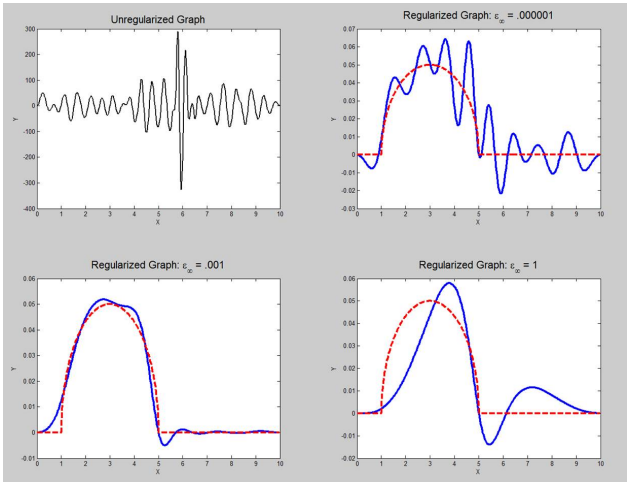

Figure 6.2: Approximations of the Curve $C(x)$ at Different Regularization Levels

As can be seen in the above figure, even a small amount of regularization helps a lot in seeing what the corrosion profile looks like. However, it is also possible to over-regularize the process, which is what has happened in the bottom right graph. With this high of a regularization coefficient, there are very few singular values left in $\mathbf{B}$, which eliminates most of the w_k functions from the final approximation of $C(x)$. With so few functions, it is impossible for the system to accurately model the curve. Since $\epsilon_\infty = 0.001$ worked well in this trial, as well as many others, that is the value used for the majority of our regularization calculations.

6.2 Variation of Input Flux

Even though our new w_k functions give a much better approximation for the curve $C(x)$, there is one major problem with them. The function will be exactly zero wherever $\frac{\partial u_0}{\partial x} = 0$. The most notable point where this is going to occur is directly under the symmetry point of the heat source. The problem with this is that no matter the choice of ϕ_k, all of the w_k functions are zero at the center of the heat source, meaning that the approximation for $C(x)$ will also go to zero there. There is no way for this method to model any corrosion at this point, or in the surrounding area because the functions are continuous. Figures 6.3 and 6.4 below show the w_k functions for a heat flux centered at $x = 5$ and the resulting $C(x)$ profile, illustrating the problem.

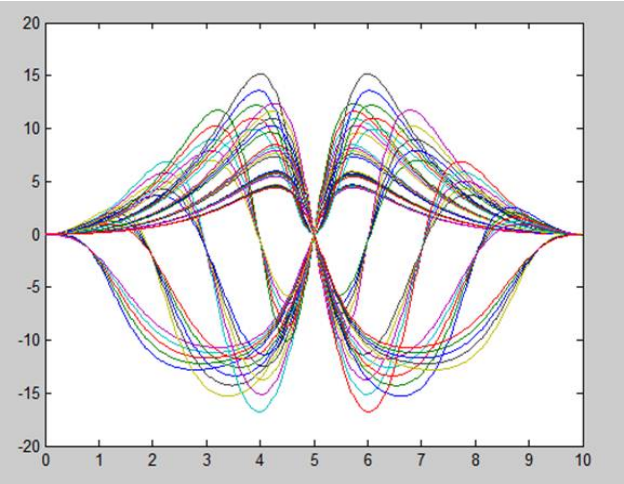

Figure 6.3: w_k Functions for a Flux Centered at 5

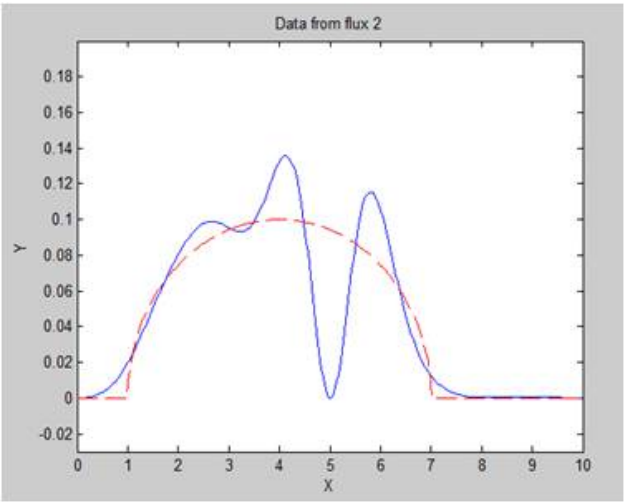

Figure 6.4: Corrosion Profile Using these w_k Functions, with an Error at 5

The way we resolved this problem was by moving the input heat flux around the plate and meshing the different solutions together. Using a time-dependent flux to move it around the plate was not met with success, so our solution was to run three separate trials for each corrosion profile. Each corrosion profile was tested with a heat flux centered at 2, 5, and 8. The three different $C(x)$ solutions were then meshed together using a set of conditional statements, ignoring each function in the interval of radius 2 around the center of the flux, with a smoothing region of .5. This set of parameters led to a smooth representation of the curve $C(x)$ that followed the actual profile fairly closely over the entire plate. Multiple images showing all three of the approximated corrosion profiles with different input fluxes, as well as the average curve, can be seen in Section 7.

7 Results

Here we show numerical examples displaying the ability of this reconstruction method to match size, location, and complication of the corrosion profile originally entered. These reconstructions were generated by setting up the corrosion profile geometry in a COMSOL file and obtaining data on the top boundary for the plate with corrosion. Another COMSOL file was used to model a plate made of the same material that had not been corroded. Data was collected from both the top and bottom boundary of this model. These files were then imported into MATLAB and the approximation for $C(x)$ was generated by the methods explained in Section 5. For all of the results, the solid line is the reconstructed profile, and the dashed line is the actual profile programmed into COMSOL. The graph in the top left is the average of the other three corrosion profiles, while the other graphs represent the individual reconstructions, with fluxes centered at 2, 5, and 8 respectively. For all of these reconstructions, the thermal parameters of material 1 are set to $k_1 = 1$ and $\alpha_1 = 1$, and the parameters for material 2 are specified under each graph. The regularization procedure and parameters of Section 6 were also used.

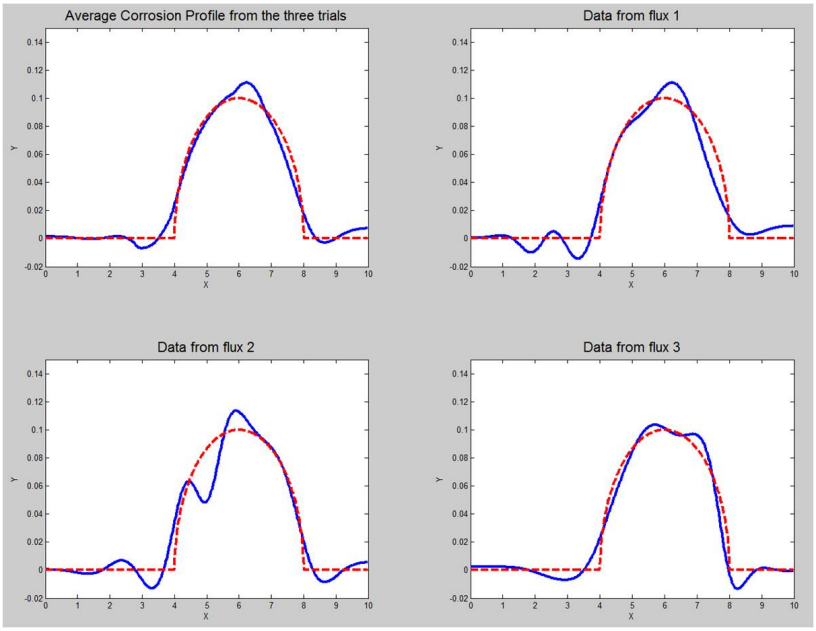

Figure 7.1: Reconstruction of Corrosion Profile with $k_2 = 0.1$, $\alpha_2 = 0.05$.

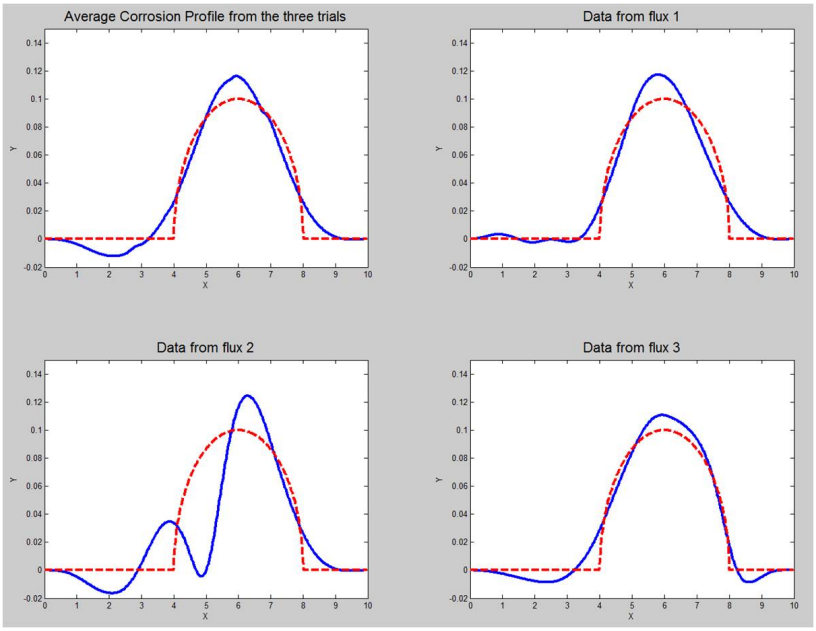

Figure 7.2: Reconstruction of Corrosion Profile with $k_2 = 0.1$, $\alpha_2 = 0.1$.

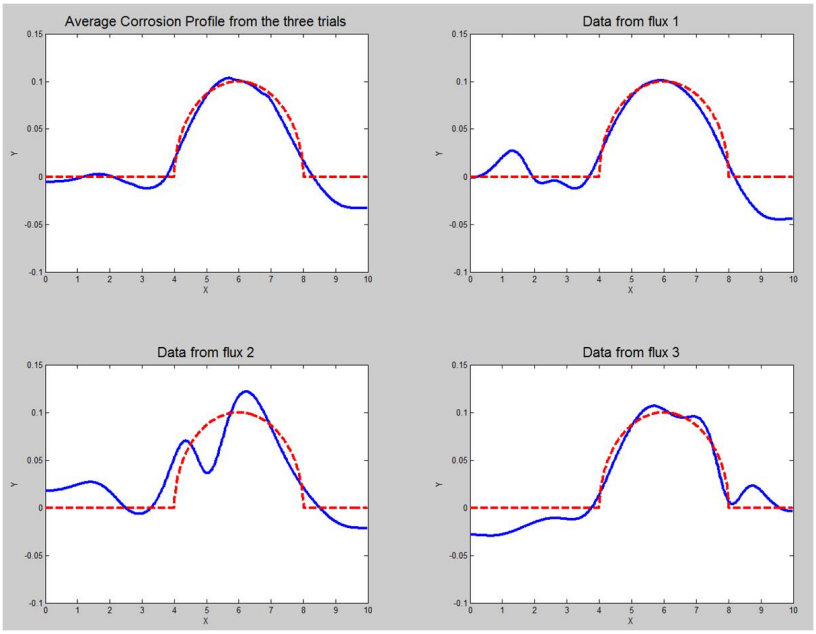

Figure 7.3: Reconstruction of Corrosion Profile with $k_2 = 0.1$, $\alpha_2 = 0.2$.

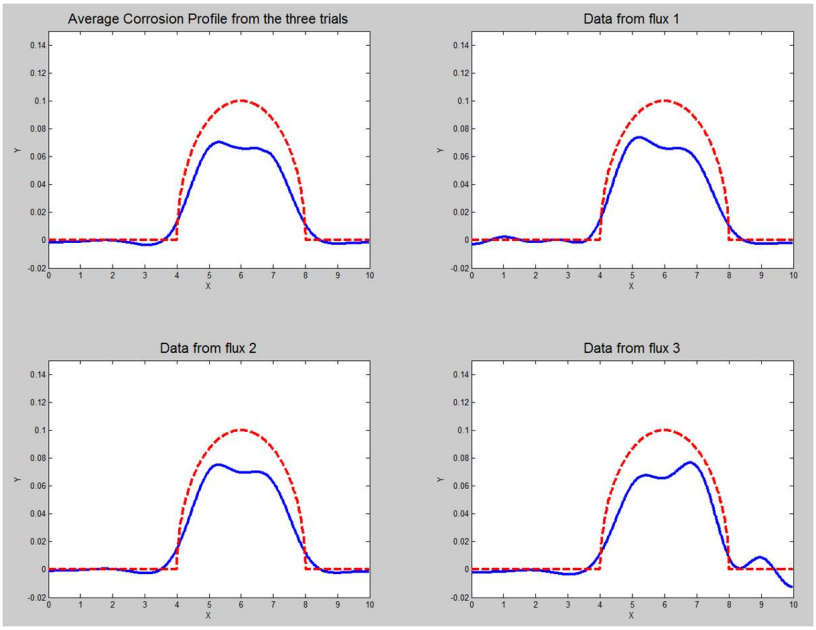

Figure 7.4: Reconstruction of Corrosion Profile with $k_2 = 1$, $\alpha_2 = 0.1$.

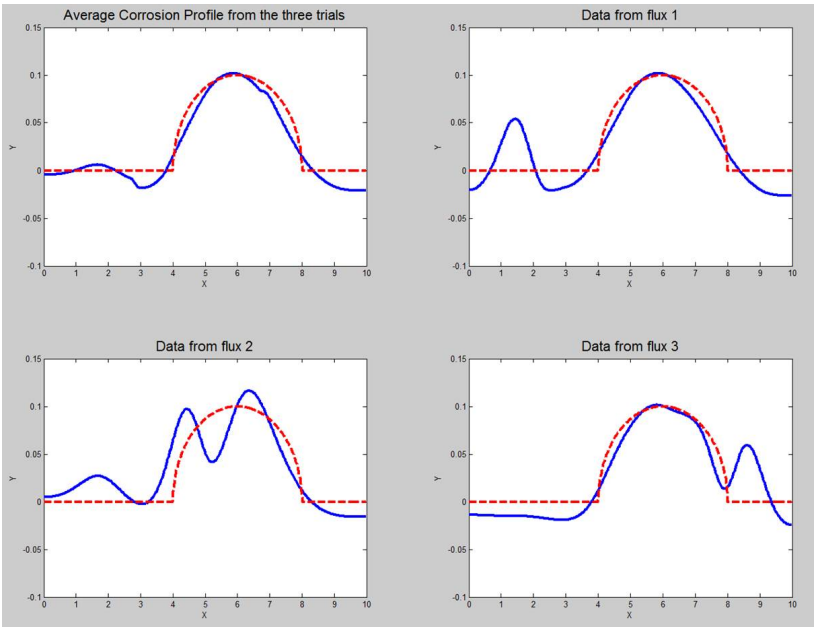

Figure 7.5: Reconstruction of Corrosion Profile with $k_2 = 0.1$, $\alpha_2 = 1$.

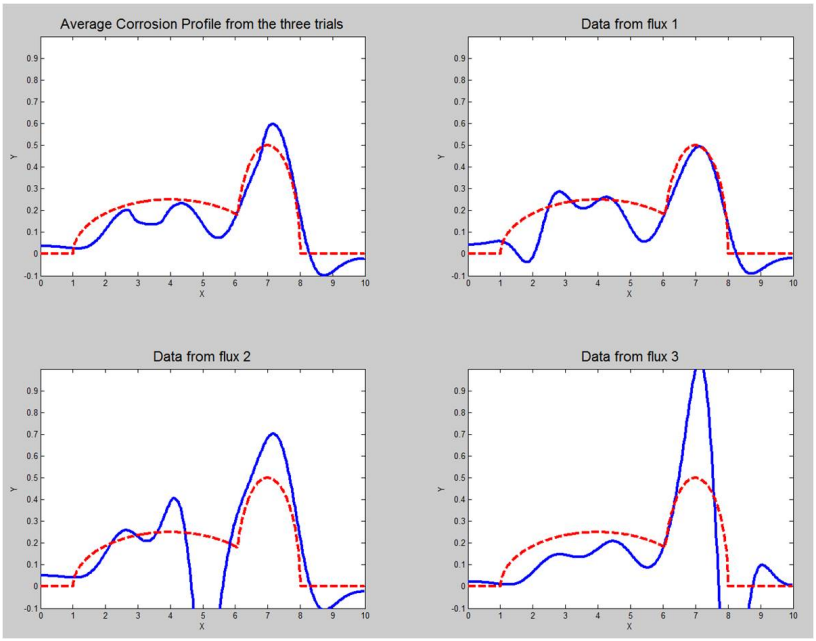

Figure 7.6: Reconstruction of Large Corrosion Profile with $k_2 = 0.1$, $\alpha_2 = 0.05$.

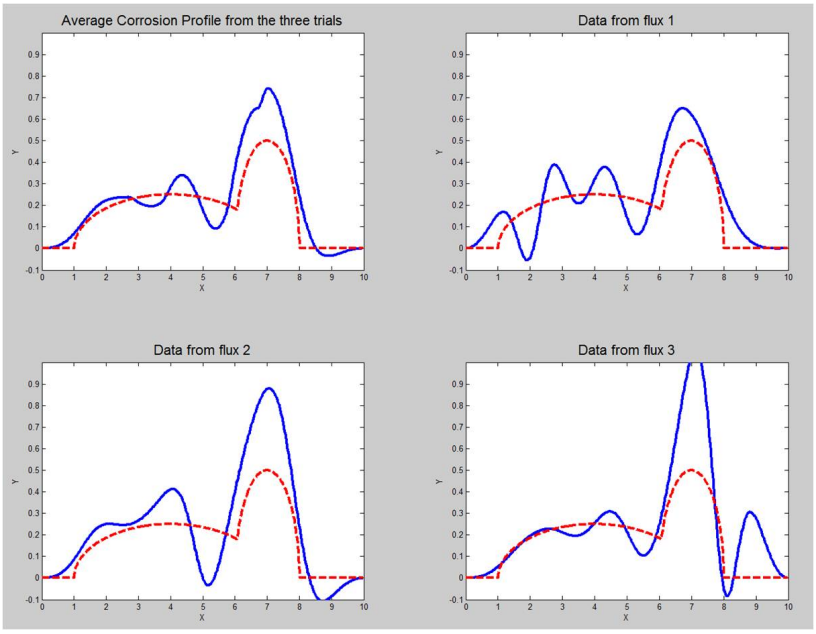

Figure 7.7: Reconstruction of Large Corrosion Profile with $k_2 = 0.1$, $\alpha_2 = 0.1$.

8 Conclusions/Discussion

As the results in Section 7 have shown, this reconstruction method allows for detection and fairly accurate imaging of plate corrosion of varying sizes with varying material parameters. If the corrosion is very small (maximum height between 1 and 10% of the plate thickness), the corrosion profile can be seen very accurately. As the corrosion size increases, the linearization assumptions are not as valid, but the reconstruction still finds the corrosion in the plate. While the height of the reconstructed profile is slightly higher than that of the actual corrosion, the location is very accurate (see Figure 7.7). Even though the overshoot is around 25% of the actual corrosion profile height, this is not necessarily a bad thing for engineering applications; seeing more corrosion than is actually there would generally cause engineers to err on the side of safety as opposed to the alternative, where seeing less corrosion results in a structural failure before it can be detected.

It has also been shown that the reconstruction process is robust under small amounts of added noise. Some noise is expected in the applications of this procedure, as thermal measuring equipment is only accurate to within a known error and the environment will cause fluctuations in the data. Gaussian noise with a mean of zero and standard deviation of 0.5% of the maximum measured temperature was applied to the temperature data recorded for the corrosion case in Figure 7.2. The corrosion profile constructed from the data with this noise was not quite as good as the reconstruction from the data without noise, but the actual corrosion profile would still be able to be recovered in an engineering situation.

The results also show, in a physical sense, the best way to image corrosion. By looking at the three individual profiles that were averaged to create the final reconstruction, it can be seen that the individual profiles that do the best at modeling the corrosion profile are the ones where the heat source is off to the side of the corrosion, and the heat is allowed to diffuse across the corrosion profile. This can be explained in several ways; the first of which can be seen in all of the results of Section 7. In that case, the w_k functions only consist of one term, which is multiplied by $\frac{\partial u_0}{\partial x}$. The issue with this term is that it is always zero at the symmetry point of the heat source, independent of the choice of ϕ. Since the w_k functions are then used as a basis to reconstruct the corrosion profile, if all of them are zero at a point, it becomes impossible for this method to 'see' any corrosion directly under the heat source. This problem was addressed using the averaging method discussed in section 6.2.

Another way this can be explained is the way in which the heat diffuses. If the heat source is on the side of the corrosion, the heat is going to diffuse over the whole plate, and thus must flow towards the corrosion profile. When it hits the corrosion profile, it can not continue forward in the same way, since there is a change in thermal conductivity at the boundary. Heat flux is preserved at the boundary, but the change in thermal conductivity will induce a change in the surrounding temperature profile. Since we have assumed the corrosion profile is a function of x, the excess heat that needs to diffuse can only move one way: up the plate towards the top edge. As the heat continues to diffuse across the plate, the corrosion profile forces more of it up towards the top of

the plate, which is where data is being gathered. Therefore, this type of trial will give a lot of information about the corrosion profile, and give the best overall reconstruction.

Another error that shows up in the reconstruction occurs when the corroded region is near the side of the plate. When this happens, the reconstruction often detects a small area of corrosion between the actual profile and the edge of the plate. This is most prevalent when the heat source is far away from the corrosion profile, and can also be explained in the same vein as the last paragraph. In this case, the heat is diffusing laterally across the corrosion profile, and is getting pushed up towards the top of the plate. When the corrosion profile becomes smaller near the edge of the plate, the heat must diffuse down to the corrosion profile in order to properly image it. However, if this is very close to the edge, the heat is unable to diffuse to the bottom of the plate at the same rate that it would normally. Therefore, the reconstruction mechanism assumes there is something there stopping it from diffusing downward, and adds corrosion to the section. This error may be systematic and could be corrected for, but that has not been completely determined as of yet.

9 Future Work

There are many possibilities for future work on the inverse problem. One of the most applicable ones is the process of converting these calculations to the three-dimensional problem. The mathematics for this problem is almost identical to the two-dimensional one discussed previously, but the computation time is greatly increased. A more efficient implementation may help with this issue, but more computing power would definitely be necessary for this to be done in a reasonable amount of time. An easier way to approach this problem might be to consider a cylindrical pipe or circular plate, as using the axisymmetric nature of the region may help to reduce calculations. The completion of the full three dimensional problem would allow for this method to be used in engineering applications to visualize corrosion.

The two dimensional problem could also be explored in a variety of different ways from here. One way is with the material and experimental parameters. In the applied case, the metals will not have thermal properties of 1 and 0.1, and the heat source will not have an arbitrary flux of 100. Consider an actual plate of steel 10 meters by 1 meter, and put the thermal conductivity and thermal diffusivity parameters for steel into COMSOL. Add in a heat flux that has been calculated from devices that would be used to apply heat in the field, and see how the plate reacts. Investigations would lead to discovering what kinds of heat fluxes are actually needed to test this procedure on physical systems and figuring out if this reconstruction can be done in an engineering sense.

Some other analysis that can be done centers around the regularization process and reconstruction of the corrosion profile. There are many other regularization methods that could be implemented, as well as other ways to pick a unique corrosion profile as a solution to the system of integral equations. In the current regularization method, the parameters ϵ_∞ and ϵ_{thresh} can be varied. Analysis could be done to see what set of these parameters work best to perform the reconstruction procedure for different sets of material parameters and corrosion profiles. All of these ideas would give a more reliable reconstruction of the corrosion profile, which could then be extended to the three dimensional case for applications.

References

[1] Court Hoang and Katherine Osenbach. *Electrical Impedance Imaging of Corrosion on a Partially Accessible 2-Dimensional Region: An Inverse Problem in Non-destructive Testing.* Rose-Hulman REU 2009

[2] Kurt Bryan and Lester Caudill. *Reconstuction of an unknown boundary portion from Cauchy data in* n *dimensions.* IOP Publishing, Inverse Problems **21** (2005) 239-255

[3] Gerald B. Folland. *Introduction to Partial Differential Equations.* Princeton University Press. October 15, 1995.

[4] Gregory F. Lawler. *Random Walk and the Heat Equation.* American Mathematical Society, 2010.

[5] Matthew Charnley and Andrew Rzeznik. *Thermal Detection of Inaccessible Corrosion.* Submitted to SIAM Undergraduate Research Online (SIURO). Preprint.